

RESEARCH ACTIVITIES IV Department of Molecular Assemblies

IV-A Solid State Properties of Phthalocyanine Salts and Related Compounds

Some phthalocyanine molecules contain unpaired d-electrons in the conjugated π -electron system. Due to this special nature, the itinerant π -electrons and localized unpaired d-electrons coexist in solid phthalocyanine salts, in which a one-dimensional double-chain system (metal and ligand chain) is formed. Furthermore these chains make up wide (π -band) and narrow (d-band) one-dimensional bands, the energy of the narrow band being close to the Fermi energy of the wide band. The phthalocyanine conductor is thus a two-chain and two-band system. These band structure and exchange interaction of itinerant π -electrons with localized magnetic moments are new aspects in the field of organic metals. For the sake of basic understanding of these materials, where a magnetic interaction takes an important role, we prepare and characterize the solid phthalocyanine salts and related compounds.

IV-A-1 Optical Spectra of the Single Crystals of Phthalocyanine Charge-Transfer Salts $\text{Co}_x\text{Ni}_{1-x}\text{Pc}(\text{AsF}_6)_{0.5}$

Yukako YONEHARA (*Grad. Univ. Adv. Stud.*) and Kyuya YAKUSHI

[*Synthetic Metals* in press]

$\text{NiPc}(\text{AsF}_6)_{0.5}$ is a two-band system, in which a narrow 3-d band is located just below the Fermi level of the wide π -band. This metallic compound undergoes a metal-insulator transition at *ca.* 50 K. On the other hand, the nearly isostructural $\text{CoPc}(\text{AsF}_6)_{0.5}$ is a non-metal already at room temperature. The different point between two compounds is the following: 3d-orbital of the central metal is singly occupied in $\text{CoPc}(\text{AsF}_6)_{0.5}$ whereas fully occupied in $\text{NiPc}(\text{AsF}_6)_{0.5}$. The polarized reflection spectra of the single crystals of $\text{Co}_x\text{Ni}_{1-x}\text{Pc}(\text{AsF}_6)_{0.5}$ ($x = 0, 0.33, 0.5, 1$) are measured in the spectral region of $600\text{--}30000\text{ cm}^{-1}$. In spite of the same band filling and isomorphous crystal structure, the reflection spectra of $\text{CoPc}(\text{AsF}_6)_{0.5}$ is quite different from all other compound as shown in Figure 1. The plasma edge at high wavenumber region and the reflectivity line shape suggests the formation of the one-dimensional band of 3d_{z²}-orbital of Co. This finding is important to understand the origin of the non-metallic nature of $\text{CoPc}(\text{AsF}_6)_{0.5}$.

At the metal-insulator transition, anomaly was found in heat capacity of $\text{NiPc}(\text{AsF}_6)_{0.5}$, which suggests the structural phase transition. Figure 2 shows that this phase transition does not accompany the usual Peierls-type lattice deformation, since the vibronic modes are not observed except the very small ones marked by arrows. The low-temperature structure analysis is necessary to understand this metal-insulator phase transition.

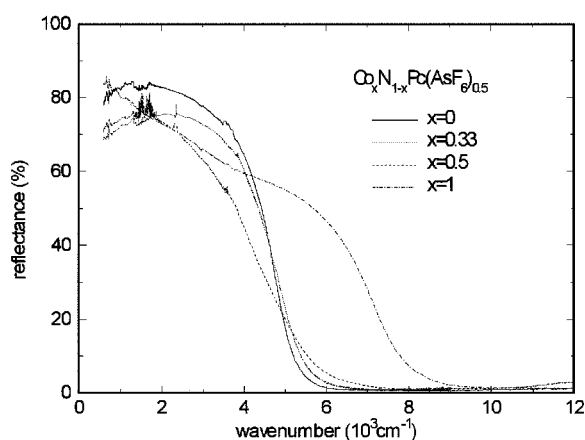


Figure 1. Reflection spectra ($//c$) of $\text{NiPc}(\text{AsF}_6)_{0.5}$, $\text{CoPc}(\text{AsF}_6)_{0.5}$, and $\text{Co}_x\text{Ni}_{1-x}\text{Pc}(\text{AsF}_6)_{0.5}$ ($x = 0.33, 0.5$). Note that $\text{CoPc}(\text{AsF}_6)_{0.5}$ demonstrates that the plasma edge is much higher than all other compounds.

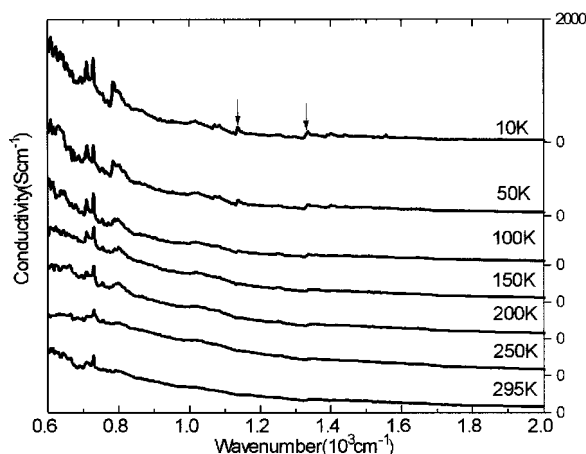


Figure 2. Temperature dependence of the $//c$ optical conductivity spectrum of $\text{NiPc}(\text{AsF}_6)_{0.5}$.

IV-A-2 Optical, EPR, and Structural Properties of Solid Platinum Phthalocyanine in the Different Oxidation States of Electrochemical Process

Yukako YONEHARA (*Grad. Univ. Adv. Stud.*), Iakov

L. KOGAN and Kyuya YAKUSHI

[*J. Electrochem. Soc.* submitted]

The electrochemical oxidation of solid platinum phthalocyanine (PtPc) was examined by cyclic voltammetry, X-ray diffraction, optical absorption, and EPR using two different samples of PtPc incorporated into transparent poly-bisphenol-A-carbonate (PBC) matrix. Two different films were used to evaluate the effect of particle size on the electrochemical and spectroelectrochemical phenomena: The film A consisted of PtPc electrochemically dispersed to nearly molecular level while the film B was formed from finely ground crystals. In the film A, the PtPc molecules were separated out from the crystal surface and distributed in the polymer matrix as a result of relatively fast scans of potentials during electrochemical pretreatment. These molecules were completely oxidized up to the dication state whereas the crystals of film B were only partially oxidized at the same anodic potential 0.8 V, limited by solvent decomposition. Initial PtPc composite film showed a one-step oxidation

in the first cycle, whereas two-step oxidation in the second and successive ones, providing the identical product at the highest oxidation state. A large constant potential difference was observed between relevant anodic and cathodic peaks with peak potentials independent of scan rate even at a very low scan rate 0.05 mVs^{-1} . The product formed after the second oxidation step was unstable in the air and transformed into the intermediate state after 24 h of exposition. EPR signal was significantly increased by changing the potential from 0.8 to -0.12 V and reduced again at -0.8 V .

Through this experiment we developed an electrochemical doping technique in solid state and identified the solid compound at each oxidation stage by X-ray diffraction. Although the band-filling control was attempted using this technique, the oxidized solid at intermediate electrochemical potential provided the superposition of the X-ray patterns of undoped and doped compounds. This means that the band-filling control by solid electrochemical method is difficult in $\text{PtPc}(\text{PF}_6)_x$.

IV-B Structure and Properties of Organic Conductors

The study of organic metals rapidly developed when the dimensionality of an intermolecular charge-transfer interaction is expanded. This expansion of dimensionality has been brought about by the discovery of new molecules such as BEDT-TTF or C_{60} . The most basic physical parameters are the transfer integrals which represent the dimensionality and itinerancy of the electron, and the on-site Coulomb energy and coupling constants with molecular vibration which represent the localized character of the electron. We systematically determine these parameters by polarized reflection spectroscopy assembling a microscope, multi-channel detection system, FT-IR, and liquid helium cryostat.

Another ongoing program is to look for negative- U organic charge-transfer compounds, the strategy of which is described in the special research project of this issue. In this research program, the most important parameter is the charge or valence of the molecule in a mixed valent state. The examination of the electronic and vibrational spectra at low temperature or high pressure is most efficient to characterize the valence. Molecular metals consisting of large or long molecules are examined by reflection and Raman spectroscopy at low temperature.

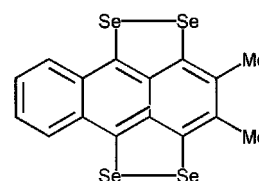
IV-B-1 Nature of the Phase Transition of Metallic DMTSA-BF₄

Jianyong OUYANG (*Grad. Univ. Adv. Stud.*), Kyuya YAKUSHI, Kazuo TAKIMIYA (*Hiroshima Univ.*) and Tetsuo OTSUBO (*Hiroshima Univ.*)

[*Synthetic Metals* in press]

A quasi-one-dimensional charge-transfer salt with a half-filled band usually becomes a Mott insulator. Because of the 1:1 chemical ratio, DMTSA-BF₄ is a half-filled band system. In contrast to this general property, DMTSA-BF₄ shows a metallic conductivity down to *ca.* 180 K and undergoes metal-insulator transition. We showed in *Annual Review 1997* that this metal-insulator transition was regarded as the Peierls transition. The temperature dependence of the $//b$ (stacking axis) spectrum was re-measured and analyzed again by plotting $\text{Re}[1/\chi''(\omega)]$. Figure 1 shows the evolution of the vibronic modes. In this figure the vibronic band appearing as a dip in $\chi''(\omega)$ is transformed into a peak. It should be noted that the vibronic modes

appear already at room temperature. This means that the breaking of the glide-plane symmetry occurs already above the metal-insulator transition temperature. This large fluctuation of the lattice distortion may be related to the one-dimensional Fermi surface of this compound. The low-temperature X-ray diffraction study is now going on. To determine the Peierls gap, the $\chi''(\omega)$ spectrum at 10 K was fitted by the one-dimensional phason model. The Peierls gap was estimated to be 140 meV which is much larger than twice the activation energies obtained by the resistivity (70 meV) and thermopower (80 meV) below 150 K.



DMTSA

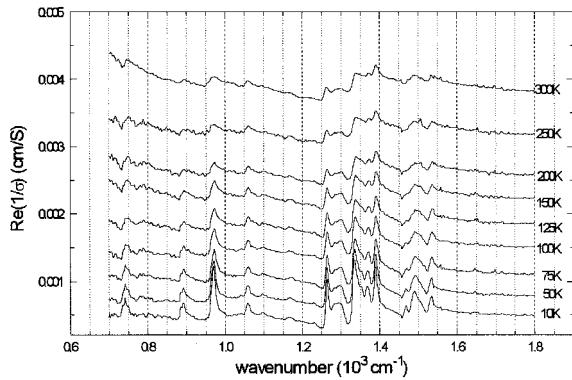


Figure 1. The evolution of the vibronic modes is shown in the plot of the real part of the inverse optical conductivity ($\text{Re}[\epsilon^{-1}(\omega)]$).

IV-B-2 Charge-Transfer Transition Polarized Perpendicular to the Molecular Stack in 1:1 Metallic DMTSA-BF₄

Jianyong OUYANG (*Grad. Univ. Adv. Stud.*), **Kyuya YAKUSHI**, **Kazuo TAKIMIYA** (*Hiroshima Univ.*), **Tetsuo OTSUBO** (*Hiroshima Univ.*) and **Hiroyuki TAJIMA** (*ISSP Univ. Tokyo*)

[*Solid State Commun.* submitted]

DMTSA is stacked along the b -axis making a zigzag chain. The neighboring molecules are overlapped in a face-to-face fashion and slid along the long molecular axis ($//b$). From this molecular arrangement, the intermolecular charge-transfer transition can occur in two polarizations: the directions of the stacking axis ($//c$) and long molecular axis ($//b$). Due to this molecular arrangement, the energy band is folded at the zone boundary making two branches. This band is filled up to this folded point. In this band model, the $//c$ optical transition is interpreted as the intra-band transition by conduction electron and the $//b$ transition as the inter-branch transition. To confirm this interpretation the inter-branch transitions are theoretically calculated based on the one-dimensional tight-binding model, and compared with the experimental observation. The optical transition from the lower filled branch to the upper branch is calculated as,

$$\begin{aligned} \sigma_{yy}(\omega) &= \frac{2i}{V\hbar^3} \langle i | [H, P_y] | f \rangle \langle f | [H, P_y] | i \rangle \frac{1}{\omega - \epsilon_{fi}} \\ &= \frac{e^2 \sqrt{2} (b)^2 t d}{\hbar^2} \frac{\sqrt{1 + \cos(2kd)}}{\omega^2 - 8t^2(1 + \cos(kd))/\hbar^2 + \omega^2} dk \end{aligned}$$

where V is the sample volume, H the tight-binding Hamiltonian i and f lower and upper half band, $\epsilon_{fi} = (E_f(k) - E_i(k))/\hbar$, V the volume of DMTSA-BF₄, b shift along the b -axis, t transfer integral, $d = c/2$. The maximum position of $\sigma_{yy}(\omega)$ gives the bandwidth, which agrees very well with the value (0.8 eV) estimated by the analysis of $\sigma_{yy}(\omega)$. We find a simple relation in the plasma frequencies or oscillator strengths of the optical transitions between the intra-band and inter-branch transitions.

$$\frac{\omega_p^2(//c)}{\omega_p^2(//b)} = d^2/(b)^2$$

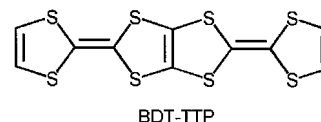
This intensity ratio 0.19 agrees well with the geometrical relation between neighboring DMTSA molecules. In this way the calculated conductivity spectrum well reproduces the observed spectrum perpendicular to the stacking axis.

IV-B-3 Two-Dimensional Band Structure of Organic Metals (BDT-TTP)₂X (X = SbF₆, AsF₆) Studied by Polarized Reflection Spectroscopy

Jianyong OUYANG, **Kyuya YAKUSHI**, **Yohji MISAKI** (*Kyoto Univ.*) and **Kazuyoshi TANAKA** (*Kyoto Univ.*)

[*J. Phys. Soc. Jpn.* in press]

Polarized reflection spectra were measured on the conductive (010) plane of metallic (BDT-TTP)₂X (X = SbF₆, AsF₆) single crystals at room and low temperatures. Well-defined plasma edges appeared in both directions parallel ($//a$) and perpendicular ($\perp a$) to the molecular stack, indicating two-dimensional band structures with a significant anisotropy. The intra- and inter-stack transfer integrals were estimated from the plasma frequencies in the framework of tight-binding model. The intra-stack transfer integral agrees very well with the value calculated by the extended Hückel approximation, whereas the inter-stack transfer integral is about half the calculated value. Based on these transfer integrals, the energy dispersion, density of state, and Fermi surface were calculated. The Fermi surfaces of both compounds were open in the k_c direction, which is different from the closed Fermi surface predicted by the extended Hückel calculation. This difference comes from the overestimation of the inter-stack transfer integrals in extended Hückel calculation. The temperature dependence of the transfer integrals was determined by analyzing the low-temperature spectra. The intra-stack transfer integral increased by about 30% whereas the enhancement of inter-stack transfer integral was very weak. So the system became more anisotropic at low temperatures. The strongly appeared CH stretching mode in the $\perp a$ spectra suggested that the conjugated π -electrons were extended over the hydrogen atoms of BDT-TTP molecule.



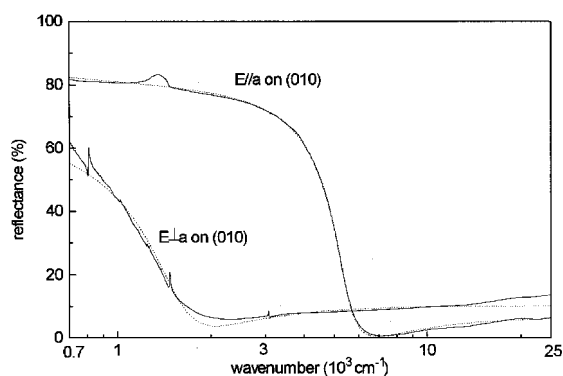


Figure 1. Polarized reflection spectrum of $(\text{BDT-TTP})_2\text{SbF}_6$. The dotted lines are the best-fit curve by Drude model.

IV-B-4 Band Structure of Organic Metal $(\text{BDT-TTP})_2\text{ClO}_4$ Studied by Polarized Reflection Spectroscopy

Jianyong OUYANG, Kyuya YAKUSHI, Yohji MISAKI (*Kyoto Univ.*) and Kazuyoshi TANAKA (*Kyoto Univ.*)

[*Synthetic Metals* in press]

Polarized reflection spectrum was measured on the conductive (100) plane of metallic $(\text{BDT-TTP})_2\text{ClO}_4$ single crystals at room and low temperatures. Well-defined plasma edges appeared in both directions parallel ($//b$) and perpendicular ($//c$) to the molecular stack, which is very similar to $(\text{BDT-TTP})_2\text{SbF}_6$. The similar spectrum comes from the similar π -type molecular arrangement although the space group is different. From the plasma frequencies, the intra- and inter-stack transfer integrals were estimated as 0.26 eV and -0.048 eV, which are almost the same as 0.26 eV and 0.048 eV for $(\text{BDT-TTP})_2\text{SbF}_6$, and 0.26 eV and 0.041 eV for $(\text{BDT-TTP})_2\text{AsF}_6$. The Fermi surfaces calculated using these transfer integrals was widely open in the k_c direction, showing the quasi-one-dimensional nature of the Fermi surface. At low temperature ρ_p ($//b$: intra-stack) increases, whereas ρ_p ($//c$: inter-stack) decreases in the same way as $(\text{BDT-TTP})_2\text{SbF}_6$ and $(\text{BDT-TTP})_2\text{AsF}_6$. This means that the system became more anisotropic at low temperatures. The strong CH stretching mode in the $//c$ spectrum is split at low temperature.

IV-B-5 Spectroscopic Study of Narrow-Band Organic Metal $(\text{BEDT-ATD})_2\text{PF}_6(\text{THF})$

Mikio URUICHI, Kyuya YAKUSHI and Yoshiro YAMASHITA

[*J. Mater. Chem.* submitted]

The polarized reflection spectrum indicates the quasi-one-dimensional band structure of $(\text{BEDT-ATD})_2\text{PF}_6(\text{THF})$, which has a narrow bandwidth of *ca.* 0.2 eV. It is surprising that such a quasi-one-dimensional narrow-band system becomes metallic. The conduction-electron absorption band of $(\text{BEDT-ATD})_2\text{PF}_6(\text{THF})$ shows two broad peaks at *ca.* 1000 cm^{-1} and

1700 cm^{-1} which feature is quite different from the Drude model. It is concluded from the crystal symmetry that a strong correlation plays an important role for this unusual absorption band profile. In the $//b$ (stacking direction) spectrum, the vibronic bands begin to grow at 100 K, which means that the screw-axis symmetry is broken below 100 K. This broken symmetry is supported by the splitting of the Raman band of a charge-sensitive vibrational mode. Unusually this structural change is not directly correlated with the thermopower and spin susceptibility which show no anomaly down to 50 K and 3 K, respectively. The intensity of some vibrational bands in the $//c$ spectrum is enhanced through the coupling with the intramolecular electronic transition at 4600 cm^{-1} . This interpretation is supported by the molecular orbital calculation of BEDT-ATD^0 .

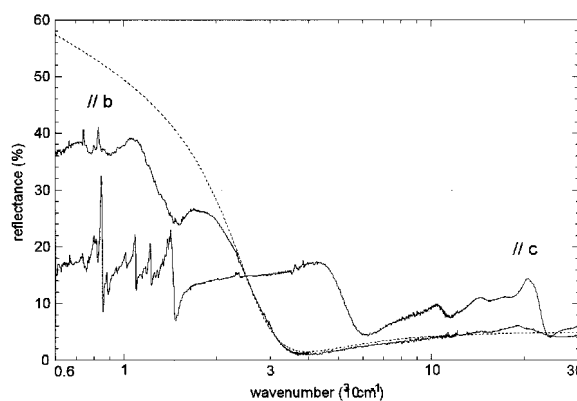
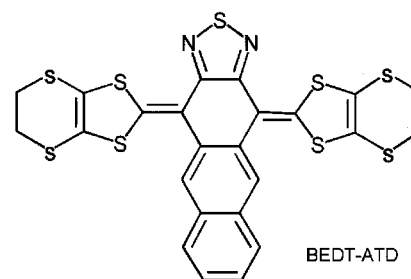


Figure 1. Polarized reflection spectrum of $(\text{BEDT-ATD})_2\text{PF}_6(\text{THF})$ measured on the (100) crystal face. The curve drawn by broken line is the Drude model fitted to the $//b$ spectrum in the region of $2500\text{-}30000\text{ cm}^{-1}$.

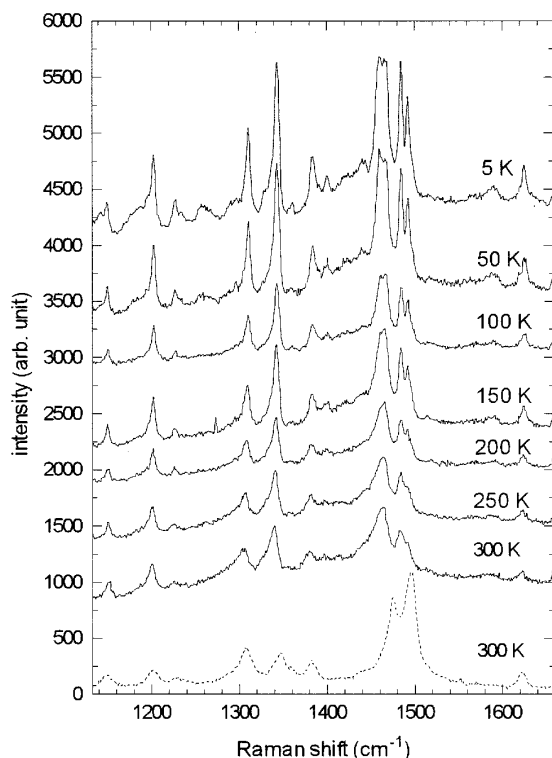


Figure 2. Temperature dependence of the Raman spectrum of $(\text{BEDT-ATD})_2\text{PF}_6(\text{THF})$ (solid lines) and BEDT-ATD^0 (broken line). One can see the softening of the C=C stretching mode by oxidation.

IV-B-6 Charge Distribution in $(\text{Et}_4\text{N})(\text{DMe-TCNQ})_2$ Crystal Studied by Raman and Reflection Spectroscopy

Chikako NAKANO, Kyuya YAKUSHI, Masayoshi KOHAMA (*Osaka Prefecture Univ.*), **Kazumasa UEDA** (*Osaka Prefecture Univ.*) and **Toyonari SUGIMOTO** (*Osaka Prefecture Univ.*)

DMe-TCNQ forms a dimerized stack in $(\text{Et}_4\text{N})(\text{DMe-TCNQ})_2$ with two crystallographically independent sites. Although the average charge of DMe-TCNQ is -0.5, the charge in different site has a different value such as -0.5+ and -0.5-. This kind of charge separation (or ordering) is sometimes accompanied by the phase transition in organic metal such as $(\text{DI-DCNQI})_2\text{Ag}$ and $(\text{BEDT-TTF})_2\text{I}_3$ and is attracting an attention as a new ground state. DMe-TCNQ is one of the compounds which have a typical charge-sensitive vibrational mode. We first examined the C=C stretching mode of DMe-TCNQ whose average charge is 0, -0.5, -0.67, and -1 and found a systematic shift. Assuming the linear relation between the shift and charge, ν was determined as 0.1. Comparison with the charge-transfer band analyzed by the polarized reflection spectrum shows that the dimer model is not sufficient to reproduce the charge separation $\nu = 0.1$. The inter-dimer charge transfer and/or relaxation by polarization effect of the CT state should be taken into account.

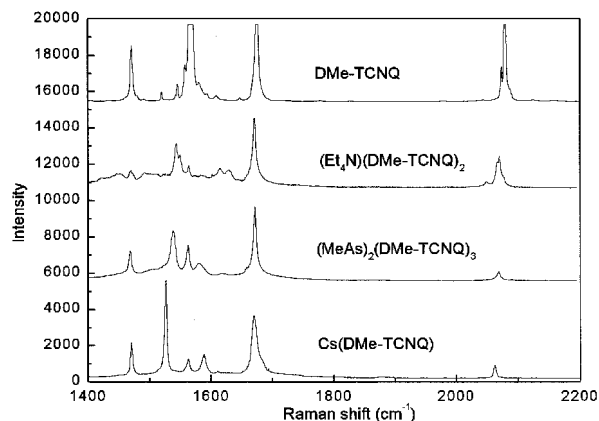
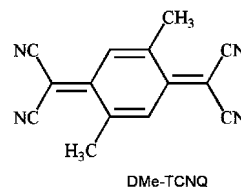


Figure 1. Raman spectra of DMe-TCNQ and its charge transfer salts with various chemical ratio.

IV-B-7 Phase Transition of $(\text{BEDT-TTF})_2\text{IBr}_2$ Studied by Polarized Reflection and Raman Spectroscopy

Makoto INOKUCHI (*Yamaguchi Science Univ. Tokyo*), **Kyuya YAKUSHI, Minoru KINOSHITA** (*Yamaguchi Science Univ. Tokyo*) and **Gunzi SAITO** (*Kyoto Univ.*)

[*Synthetic Metals* in press]

The molecular semiconductor $(\text{BEDT-TTF})_2\text{IBr}_2$ is known to undergo structural phase transition at 200 K and magnetic phase transition at 60 K. In the $(\text{BEDT-TTF})_2\text{IBr}_2$ spectrum, the broad band around 1200 cm^{-1} of the electronic origin abruptly decreased below 200 K, and at the same time the interference pattern is observed. The appearance of the interference pattern means that the spectral region below 1500 cm^{-1} becomes transparent, which suggests the increase of the charge gap. No change is observed at 60 K. It is well known that $\nu_3(\text{ag})$ mode of BEDT-TTF is sensitive to the charge or valence and a sharp Raman band is observed at $1460\text{--}1470\text{ cm}^{-1}$ in $\text{BEDT-TTF}^{0.5+}$. A broad Raman band is observed at room temperature around $1470\text{--}1480\text{ cm}^{-1}$ in the corresponding spectral region. This band begins to split at 210 K, each component is well separated (1454 cm^{-1} and 1490 cm^{-1}) at 180 K, and high-wavenumber component shows a shoulder (1484 cm^{-1}) at 5.4 K. This spectral feature indicates that the charge on the four BEDT-TTF molecules in the unit cell has some distribution around +0.5 at room temperature and this charge separation (disproportionation) is fixed below the structural phase transition at 200 K.

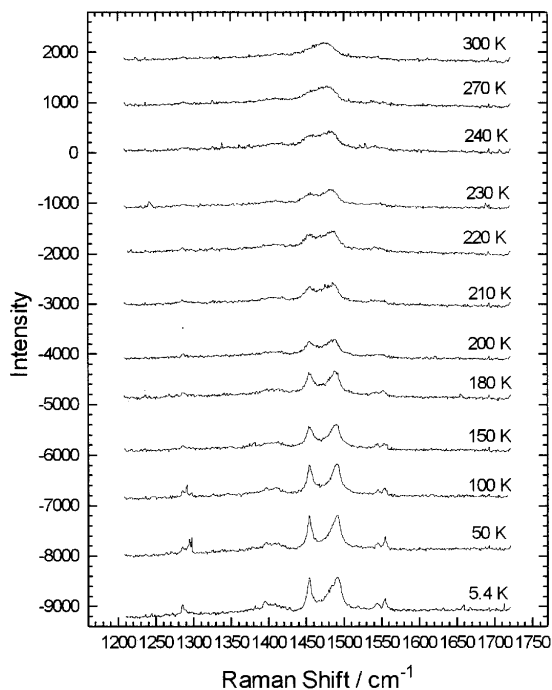


Figure 1. ν_3 mode in Raman spectrum of β' -(BEDT-TTF) $_2$ IBr $_2$

IV-B-8 BEDT-TTF Being Inserted into a Layered MnPS $_3$

Chuluo YANG (Wuhan Univ.), Jingui QIN (Wuhan Univ.), Kyuya YAKUSHI, Yasuhiro NAKAZAWA and Kenji ICHIMURA (Kumamoto Univ.)

[Synthetic Metals in press]

BEDT-TTF was inserted into the layered MnPS $_3$ by ion exchange reaction of a new pre-intercalate Mn $_{0.86}$ PS $_3$ (bipy) $_{0.56}$ with (BEDT-TTF) $_2$ I $_x$, affording a novel inorganic-organic nano-composite material, the intercalate Mn $_{0.86}$ PS $_3$ (ET) $_{0.46}$. The expansion of the lattice spacing is the largest in the intercalates based on MPS $_3$ so far. It shows a conductivity (on compressed pellet) 10^5 times higher than that of the pristine MnPS $_3$. Contrary to the ferromagnetic phase transition in Mn $_{0.86}$ PS $_3$ (bipy) $_{0.56}$, which was synthesized by us before, this new intercalate did not show any magnetic transition.

IV-C Thermodynamic Study of Organic Conductors

In order to get reliable information on the electron density of states and on the entropy distribution around the phase transition, specific heat studies are inevitable. In this project, we aim at constructing several types of calorimeters available at low-temperature region and also in magnetic fields and performing systematic investigation on organic materials from a thermodynamic viewpoint.

IV-C-1 Thermodynamics of BEDT-TTF Based Dimeric Salts

Yasuhiro NAKAZAWA and Kazushi KANODA (Univ. Tokyo)

[Synth. Metals Submitted]

The low-temperature electronic properties of 2:1 salts of BEDT-TTF molecules are studied by specific heat measurements, especially focusing on the dimeric systems. It is recently pointed out that when the intradimer coupling becomes larger than other overlap integrals in the BEDT-TTF layers as is typically the case of β' - and β -type salts, a dimerization gap appears in the center of HOMO band and consequently it splits into upper-HOMO and lower-HOMO bands. The quarter-filled state of holes provided by the monovalence of anions is therefore considered as an effectively half-filled state of the upper-HOMO band. The degree of dimerization is, therefore, considered as an important parameter to control the electron correlation in this type of compounds. The C_p/T vs T^2 curves of β' -(BEDT-TTF) $_2$ Cl $_2$ and the insulating salts of β -type structure are shown in Figure 1. The absence of T-linear temperature dependence at low-temperature region demonstrates that the Mott insulating behavior is manifested itself in their electronic ground states of this material, which is consistently understood with the above picture.

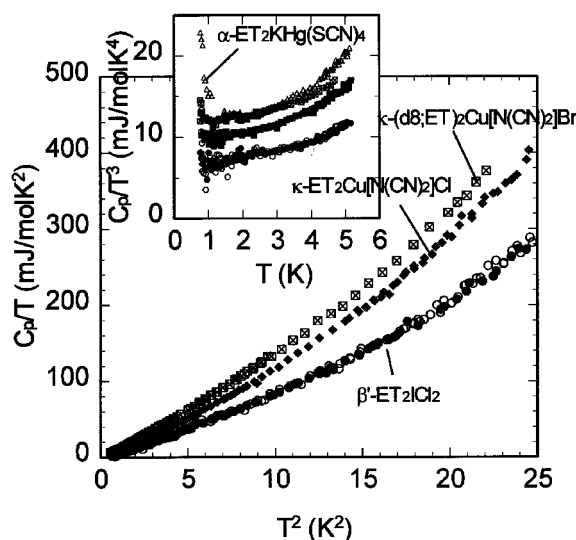


Figure 1. C_p/T vs T^2 plot of insulating salts of (BEDT-TTF) $_2$ X. The inset shows C_p/T^3 vs T plots.

IV-C-2 Cooling Rate Dependence of Low-Temperature Specific Heat of Deuterated β -(BEDT-TTF) $_2$ Cu[N(CN) $_2$]Br

Yasuhiro NAKAZAWA and Kazushi KANODA (Univ. Tokyo)

We report the result of low-temperature specific

heat measurements of deuterated $-(\text{BEDT-TTF})_2\text{Cu}[\text{N}(\text{CN})_2]\text{Br}$, which is situated at the critical region of the Mott transition between superconductive phase and insulating phase of $-(\text{BEDT-TTF})_2\text{X}$ system by changing cooling rate to control the volume fraction of superconductive and insulating phases. The electronic specific heat contribution do not show distinct variation by changing cooling rate from 0.07 K/min to 50 K/min. The magnetic fields dependence of the electronic specific heat is also studied up to 6T as is shown in Figure 1. Here, we do not observe drastic increase of term in the present accuracy of the measurement. This fact demonstrates that the density of superconducting electrons in this material, even if they exist, is smaller than those of superconducting material of hydrogenated $\text{X} = \text{Cu}[\text{N}(\text{CN})_2]\text{Br}$ and $\text{Cu}(\text{NCS})_2$ salt.

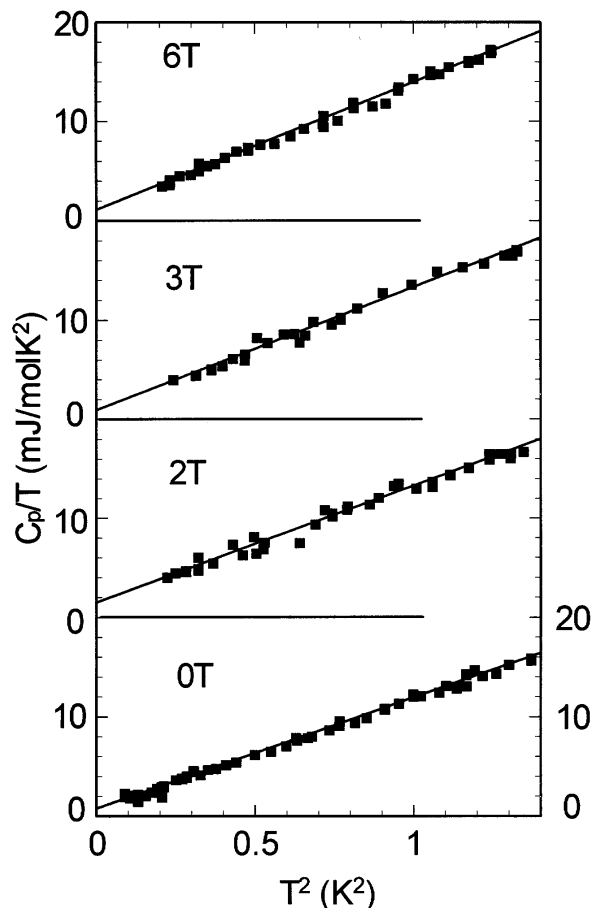


Figure 1. Magnetic field dependence of low-temperature specific heat of $-(d_8;\text{BEDT-TTF})_2\text{Cu}[\text{N}(\text{CN})_2]\text{Br}$ cooled down with the rate of 0.8 K/min.

IV-D Photoelectron Spectroscopy of Organic Solids in Vacuum Ultraviolet Region

The works of ultraviolet photoelectron spectroscopy (UPS) and also of UPS with synchrotron radiation lightsource (UVSOR-UPS) of organic materials have been proceeded to find their quantitative electronic structures.

IV-D-1 Origin of the Photoemission Intensity Oscillation of C_{60}

Shinji HASEGAWA, Takayuki MIYAMAE, Kyuya YAKUSHI, Hiroo INOKUCHI, Kazuhiko SEKI (Nagoya Univ.) and **Nobuo UENO** (Chiba Univ.)

[Phys. Rev. B **58**, 4927 (1998)]

The photon energy dependences of photoemission intensities of C_{60} were quantitatively calculated by the single-scattering approximation for the final state and the *ab-initio* molecular orbital calculation for the initial state. The calculated results agreed well with the measured intensity oscillation in the photon energy range of $h\nu = 18\text{--}110$ eV. The calculation by the plane-wave approximation for the final state also gave the similar oscillations, which suggests that the oscillations are independent of the accuracy of the final state. These results indicated that the oscillations originate from the

interference of photoelectron waves emanating from the 60 carbon atoms, *i.e.*, the multi-centered photoemission with the phase difference of each wave. Further, the analytical calculation with a simplified spherical-shell like initial state revealed that the spherical structure of C_{60} molecule and its large radius dominate the oscillations.

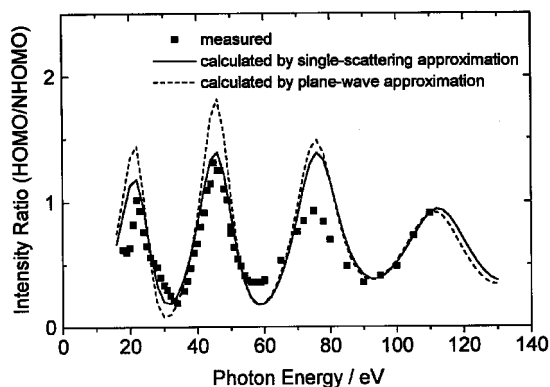


Figure 1. Photon energy $h\nu$ dependences of photoemission intensity ratio of HOMO/NHOMO. The intensity oscillation of the measured results (solid squares) is in good agreement with the calculated curves. The solid line was calculated by the single-scattering approximation for the final state. The broken line was calculated by the plane-wave approximation for the final state. The initial state calculated by STO-5G MO method was used for both calculations.

IV-E Electrical Conduction and its Related Properties of Organic Solids

Two major categories of organic solids are known to offer the prospect of good electrical conduction. The first group comprises single-component materials; typical examples are polycyclic aromatic compounds and also phthalocyanines. The second group consists of charge-transfer complexes such as the perylene-bromine complexes (donor-acceptor complexes). After the accumulation of large number of works on those charge-transfer complexes, their conductivity ranges from semiconductivity to superconductivity.

To expand the research field of molecular conductors, we always consider to introduce a new category. Recently, with the introduction of gaseous elements such as hydrogen and nitrogen to the charge-transfer complexes, we are finding the third category to produce a new type of molecular conductors: Three components organic semiconductors.

In this section, therefore, we present the works on the electronic properties of single component organic semiconductors, charge-transfer complexes and also three components organic superconductor based on C_{60} . We summarize the work of molecular fastener as review article.

IV-E-1 Molecular Fastener

Hiroo INOKUCHI

A series of tetrakis (alkylthio)-tetrathiafulvalenes (TTC_n -TTF) has been prepared. These compounds constitute novel type of single component organic semiconductors. The electrical resistivities of those single crystals have been measured in a vacuum of 10^{-6} Torr; the room temperature dark resistivity reaches 10^5 cm, a value that is extraordinarily low compared with those of ordinary organic semiconductors constructed with a single component. The cause of this low resistivity is close packing of molecules in crystal. From the crystal structural analysis, the shortest distance between sulfur atoms of central tetrathio-tetrathiafulvalene skeleton in two adjacent molecules has been found to be 3.57 Å for TTC_9 -TTF and TTC_{10} -TTF, which is considerable shorter than the sum of the van der Waals radius (3.70 Å). The central skeleton has been "fastened" strongly with the substituted four long alkyl chains. We call this type of organic

semiconductors by the name of "Molecular Fastener".

IV-E-2 Na-X- C_{60} (X = N, H) Superconductors

Kenichi IMAEDA and Hiroo INOKUCHI

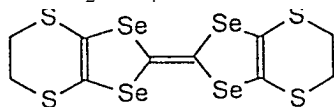
[*Trends in Chem. Phys.* 5, 239 (1997)]

We found superconductivity in the sodium-X- C_{60} (X = nitrogen and hydrogen) ternary compounds. The onset T_c is observed at 13 K for $Na_xN_yC_{60}$ and 15 K for $Na_xH_yC_{60}$. In contrast to $Na_xN_yC_{60}$ composed of two face-centered-cubic (fcc) phases, $Na_xH_yC_{60}$ crystallizes in a single fcc phase. The Rietveld analysis for the powder X-ray diffraction pattern of $Na_xH_yC_{60}$ demonstrates that Na^+ ions in both the tetrahedral and octahedral sites are off-centered. Hydrogen in $Na_xH_yC_{60}$ is detected by solid state 1H NMR and thermal desorption spectroscopy. $Na_xN_yC_{60}$ and $Na_xH_yC_{60}$ superconductors containing off-centered alkali-metal ions belong to the different family from the on-centered M_3C_{60} and Na_2MC_{60} .

IV-F Superconductivity and Antiferromagnetism of β -Type BETS Conductors

Since the discovery of the semiconducting properties of molecular solids such as phthalocyanine and aromatic hydrocarbons around 1950, conducting properties of a vast of organic conductors have been studied and a great progress has been achieved in the field of organic conducting systems. The widely accepted clear evidences

showing the existence of the metal electrons in molecular crystals was obtained in the early 1970's and the first organic superconductor was reported in 1980. In addition, the first molecular superconductor based on transition metal complex molecules was discovered in 1986 and the first paramagnetic organic superconductor was reported in 1995. On the other hand, despite of the increasing number of the organic superconductors, the speed of the essential progress in the development of organic superconductors seems to be slowing down recently. For example, the highest T_c record of organic superconductors has been stopped almost 10 years since the discovery of β -BEDT-TTF $_2$ Cu[N(CN) $_2$]Cl in 1990. We have examined a series of BETS (= bis(ethylenedithio)tetraselenafulvalene) conductors with tetrahalide anions, β -BETS $_2$ Fe $_x$ Ga $_{1-x}$ Br $_y$ Cl $_{4-y}$. Our main interest is in the development of new conducting systems by incorporating Fe $^{3+}$ magnetic anions. Of course the above-mentioned first paramagnetic superconductors is an excellent example of the magnetic organic conductors but the magnetic ions in this system was revealed to be almost independent of the conduction electrons. We have recently discovered an unprecedented superconductor-to-insulator transition in β -type BETS conductors. To our knowledge, such a transition has not been observed in the inorganic superconductors. In addition, we have found the superconductor-to-metal transition. The Fe $^{3+}$ ions play an essential role in breaking superconductivity. It may be said that a new class of organic superconductors with non-superconducting ground states has been discovered after two decades of the first report of the organic superconductor. Furthermore, we have discovered the evidence for the first antiferromagnetic organic metal phase in β -BETS $_2$ FeCl $_4$.



BETS (= bis(ethylenedithio)tetraselenafulvalene)

IV-F-1 Evidence of the Bulk Superconductor-to-Insulator Transition in β -BETS $_2$ Fe $_x$ Ga $_{1-x}$ Cl $_4$ ($x = 0.45$)

Hayao KOBAYASHI, Akane SATO, Emiko ARAI, Yasuhiro NAKAZAWA, Akiko KOBAYASHI (Univ. Tokyo) and Patrick CASSOUX (CNRS)

We have recently discovered a novel superconductor-to-insulator transition in β -BETS $_2$ Fe $_x$ Ga $_{1-x}$ Cl $_4$ ($x = 0.45$). The resistivity measurements on the system with $x = 0.43$ showed a superconducting transition around 4.2 K and a subsequent superconductor-to-insulator (SC-I) transition around 3 K. Since such drastic conducting phenomena have never been observed even in the inorganic systems, the microscopic mechanism of the transition will be of great interest. We have already reported the anomalous susceptibility behavior around T_{SC-I} . However we found recently the reported susceptibility was not correct for the weak field perpendicular to the needle axis of the crystal ($H \perp c$) because of the "effective pressure" produced by the freezing of the grease used to keep the crystals in the glass capillary. Therefore we reexamined the susceptibility of two samples of oriented thin needle crystals very carefully. A sharp drop of the susceptibility and its recovery at lower temperature clearly showed that the crystal once transforms into superconducting state and returns to the non-superconducting state. In order to estimate the superconducting volume fraction, we measured the *ac* susceptibility and found the Meissner volume fraction to be about 75% at 4 K, which showed conclusively the bulk nature of the SC-I transition (Figure 1).

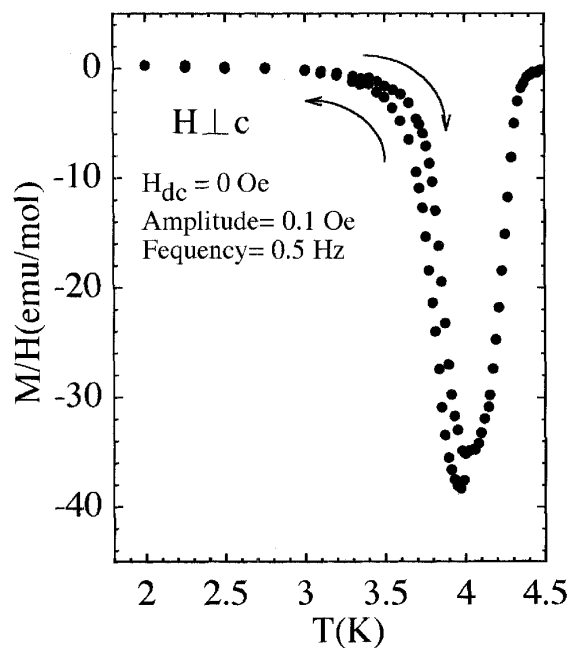


Figure 1. The *ac* susceptibility of β -BETS $_2$ Fe $_x$ Ga $_{1-x}$ Cl $_4$ ($x = 0.45$)

IV-F-2 Superconductor-to-Metal Transition in β -BETS $_2$ Fe $_x$ Ga $_{1-x}$ BrCl $_3$ ($x = 0.1-0.2$)

Hayao KOBAYASHI, Hisashi TANAKA (Univ. Tokyo), Akiko KOBAYASHI (Univ. Tokyo) and Patrick CASSOUX (CNRS)

As reported before, we have found the superconductor-to-insulator (SC-I) transition in β -BETS $_2$ Fe $_x$ Ga $_{1-x}$ Cl $_4$ ($x = 0.45$). We have also examined the resistivity of Br-containing systems β -BETS $_2$ Fe $_x$ Ga $_{1-x}$ BrCl $_3$. It has been reported that the exchange of Cl atoms to Br atoms produces the effectively "negative pressure" in the crystal. At ambient pressure, the crystal

showed the semiconducting behavior down to low temperature. But at high pressure, it exhibited the SC-I transition ($x = 0.5$ around 2 kbar) or the SC-M transition ($x = 0.1-0.2$ around 1.5 kbar): $T_c = 7$ K, T_{SC-I} or $T_{SC-M} = 3.5-4$ K (Figure 1). It may be said that the breaking of superconductivity occurs irrelevantly the nature of the ground state (metallic state or insulating state). Since the superconducting states of all the α - $BETS_2GaBr_{1-x}Cl_{4-x}$ systems without Fe^{3+} ions are stable down to low temperature, it is clear that Fe^{3+} ions play crucial role in breaking the superconductivity. At higher pressure, the system showed a simple superconducting behavior and then became a stable metal down to low temperature.

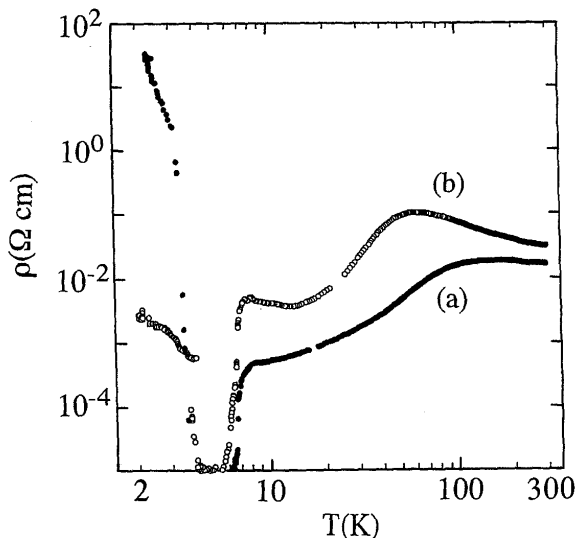


Figure 1. SC-M and SC-I transitions of α - $BETS_2Fe_xGa_{1-x}BrCl_3$. (a) $x = 0.2$ (b) $x = 0.5$

IV-F-3 Temperature-Composition Phase Diagram of α - $BETS_2Fe_xGa_{1-x}Cl_4$

Akane SATO, Emiko OJIMA, Hiroki AKUTSU, Hayao KOBAYASHI, Akiko KOBAYASHI (Univ. Tokyo) and **Patrick CASSOUX** (CNRS)

[Chem. Lett. 673 (1998)]

In order to determine the phase diagram of α - $BETS_2Fe_xGa_{1-x}Cl_4$, the preparation, EPMA (electron probe microanalysis), resistivity measurements of α - $BETS_2Fe_xGa_{1-x}Cl_4$ were made systematically. The crystals were grown electrochemically from the 10% ethanol-containing chlorobenzene solutions of BETS, $[(C_2H_5)_4N]FeCl_4$ and $[(C_2H_5)_4N]GaCl_4$. The Fe-rich system showed a sharp metal-insulator transition and the transition temperature (T_{MI}) decreased with decreasing Fe-content (x). In the Ga-rich system, the superconducting transition was observed. The T_c decreased with increasing x . The SC-I transition was observed at $x = 0.35-0.5$ (Figure 1). From the spin flop behavior and the anisotropy of the susceptibilities of the system exhibiting a M-I transition ($x = 1.0, 0.7, 0.55$) or a SC-I transition ($x = 0.45$), it was concluded that the system takes a characteristic d -coupled antiferromagnetic insulating ground state at $x > 0.35$.

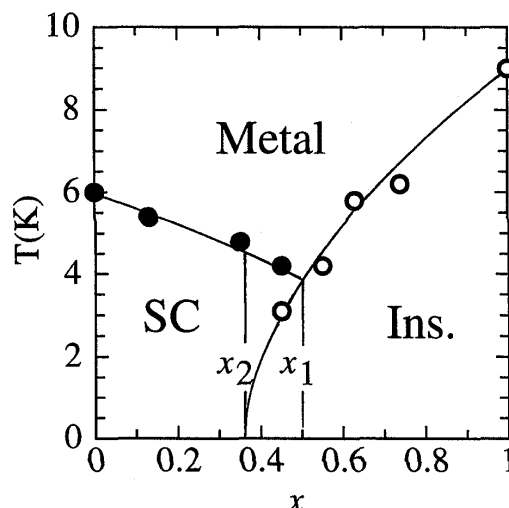


Figure 1. Temperature-composition phase diagram of α - $BETS_2Fe_xGa_{1-x}Cl_4$

IV-F-4 Antiferromagnetic Ordering of Diluted Fe^{3+} Spins in α - $BETS_2Fe_xGa_{1-x}BrCl_3$ ($x = 0.1$)

Hisashi TANAKA (Univ. Tokyo), **Akiko KOBAYASHI** (Univ. Tokyo), **Hayao KOBAYASHI, Akane SATO and Patrick CASSOUX** (CNRS)

The physical properties of α -type BETS conductors can be controlled continuously by exchanging the metal atoms (Fe, Ga) and/or halogen atoms (Br, Cl). We have recently examined the susceptibility of α - $BETS_2Fe_xGa_{1-x}BrCl_3$ ($x = 0.1-0.2$), which exhibits a semiconducting property at ambient pressure and superconducting-to-metal (SC-M) transition around 1.5 kbar. Quite unexpectedly, only 10% Fe^{3+} spins showed antiferromagnetic ordering below ca. 4 K. The spin-flop behavior was observed around 1.5 T for the field perpendicular to c (Figure 1). In the successive SC and SC-M transitions around 1.5 kbar, Fe^{3+} ion will play an important role. Since the free energy of superconducting state becomes lower than that of the metallic state at T_c ($= 7$ K), the low-temperature metallic state below T_{SC-I} ($= 3.5$ K) is considered to be more stable than the high-temperature metallic state above T_c . One possible mechanism of the stabilization of the low-temperature metallic state will be related to the antiferromagnetic ordering of Fe spins, which seems to coexist with metallic state but not with superconducting state.

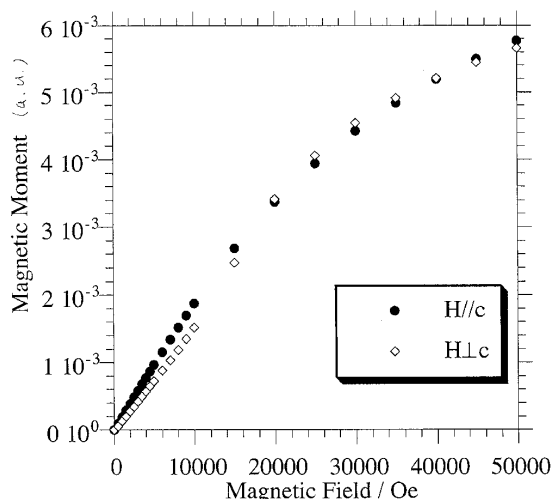


Figure 1. Magnetization of $-\text{BETS}_2\text{Fe}_x\text{Ga}_{1-x}\text{BrCl}_3$ ($x = 0.1$) at 3 K

IV-F-5 The x -Dependence of Antiferromagnetic Interaction between Fe^{3+} Ions in $-\text{BETS}_2\text{Fe}_x\text{Ga}_{1-x}\text{Cl}_4$

Akane SATO, Emiko OJIMA, Hayao KOBAYASHI, Akiko KOBAYASHI (*Univ. Tokyo*) and Patrick CASSOUX (*CNRS*)

The role of Fe^{3+} spins is a key factor to understand the anomalous conducting properties of $-\text{BETS}_2\text{Fe}_x\text{Ga}_{1-x}\text{Cl}_4$. ESR and SQUID measurements showed the antiferromagnetic interaction between localized Fe spins. Since the shortest Fe...Fe distance is longer than 6 \AA , the dipole-dipole interaction between Fe^{3+} spins is very small and therefore Fe-Fe interaction must be mediated by electrons of BETS molecules. Since the Fe and Ga atoms seem to be almost ideally mixed in the crystals, the detailed studies on the magnetic interaction between diluted Fe spins in two-dimensional conducting system will be possible in $-\text{BETS}_2\text{Fe}_x\text{Ga}_{1-x}\text{Cl}_4$, which is very difficult in the usual organic conducting systems. Weiss temperature of $-\text{BETS}_2\text{Fe}_x\text{Ga}_{1-x}\text{Cl}_4$ decreases with decreasing x ($\theta = -8\text{K}$ at $x = 1.0$) at $x > 0.35$, where the system takes insulating ground state and tends to be constant ($\theta = -1.8\text{K}$) below 0.35 , where a simple superconducting transition is observed.

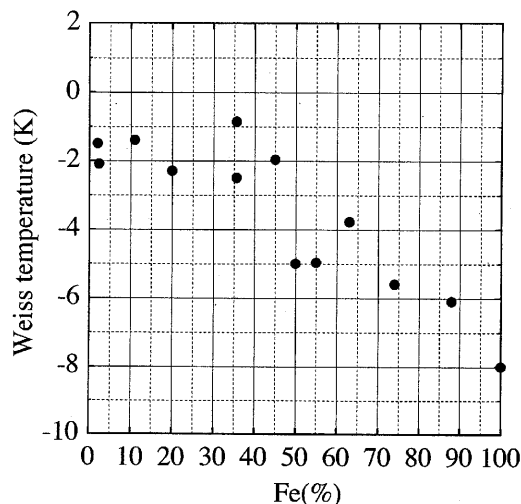


Figure 1. The x -dependence of Weiss temperature of $-\text{BETS}_2\text{Fe}_x\text{Ga}_{1-x}\text{Cl}_4$.

IV-F-6 Easy Axis Rotation of Antiferromagnetic Structure and Phase Diagram of $-\text{BETS}_2\text{FeBr}_x\text{Cl}_{4-x}$

Hiroki AKUTSU, Kiyonori KATO, Emiko OJIMA, Hayao KOBAYASHI, Hisashi TANAKA (*Univ. Tokyo*), Akiko KOBAYASHI (*Univ. Tokyo*) and Patrick CASSOUX (*CNRS*)

[*Phys. Rev. B* in press]

The electric and magnetic properties of a series of highly correlated two-dimensional organic conductors incorporating magnetic ions (Fe^{3+} with $S=5/2$), $-\text{BETS}_2\text{FeBr}_x\text{Cl}_{4-x}$ ($x = 0-0.8$) were examined by controlling the Br content (x). A broad resistivity maximum at 100K ($x = 0$) - 50K ($x = 0.7$) indicating the strong correlation of σ -conduction electrons becomes prominent with increasing x . At the same time the metal-insulator (MI) transition temperature (T_{MI}) was enhanced from 8.5K ($x = 0$) to 18K ($x = 0.7$). At $0 < x < 0.2$, the MI transition and the antiferromagnetic (AF) transitions took place cooperatively around 8.5 K ($T_{\text{N}} = T_{\text{MI}}$). A large magnetization drop was observed at T_{MI} for the magnetic field parallel to c axis ($H//c$), which indicates the appearance of localized σ spins ($S=1/2$) and the strong AF coupling of σ and d spin systems. At $0.3 < x < 0.5$, two anomalies were observed in the magnetization-temperature (M - T) curve. The high-temperature anomaly corresponds to MI transition (T_{MI}) and the low-temperature one corresponds to AF ordering of the Fe^{3+} spins (T_{N}). For $x > 0.6$, the magnetization drop at T_{MI} disappeared, which shows that the σ electron system undergoes MI transition independently of the d spin systems. The disappearance of the susceptibility anomaly at T_{MI} indicates that the electron system transforms to non-magnetic insulating state below T_{MI} . On the other hand, the anisotropy of M showing the development of AF spin structure of Fe spins was observed independently of x ($0 < x < 0.8$). Around $x = 0.3-0.5$, the direction of easy axis of the AF spin structure changes from parallel to c ($x < 0.2$) to perpendicular to it ($x > 0.6$). In other words, the

direction of easy axis is varied according to the magnitude of d -coupling. The Weiss temperature (θ) determined from the M - T curve at $T_{MI} < T < 30K$ decreased with increasing x .

IV-F-7 Systematic x -Dependence of the Crystal Structure and Magnetic and Electric Properties of $\text{-BETS}_2\text{GaBr}_x\text{Cl}_{4-x}$

Hisashi TANAKA (*Univ. Tokyo*), **Akiko KOBAYASHI** (*Univ. Tokyo*), **Akane SATO**, **Hiroki AKUTSU** and **Hayao KOBAYASHI**

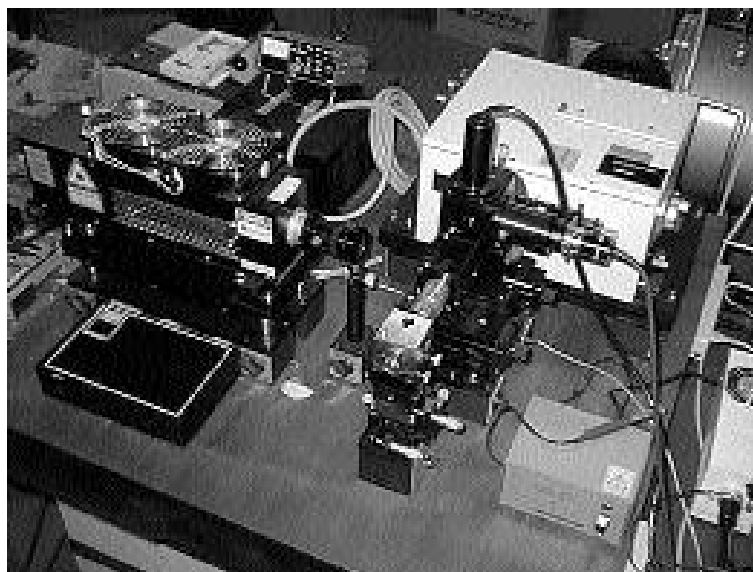
The electrical transport properties of $\text{-BETS}_2\text{GaBr}_x\text{Cl}_{4-x}$ ($0 < x < 2$) are drastically changed by varying bromine content x and/or applying pressure. At ambient pressure, the superconducting transition could be observed at $x < 0.75$. The pressure and x dependencies of T_c were examined. The M - H curve of $\text{-BETS}_2\text{GaCl}_4$ at 2K indicated the almost perfect Meissner state of superconducting phase (M = magnetization; H =

magnetic field). The H_{c1} is about 8 Oe for $H \parallel c$ and 12 Oe for $H \perp c$. The magnetic susceptibility of $\text{-BETS}_2\text{-GaBr}_x\text{Cl}_{4-x}$ increases with decreasing temperature down to about 60K, below which the susceptibility becomes x -dependent and tends to be suppressed with increasing x . The isotropic decrease of the susceptibility at lower temperature observed in the insulating system with $x > 1.1$ indicates the insulating ground state to be not antiferromagnetic but probably non-magnetic. The crystal structure determinations of a series of $\text{-BETS}_2\text{-GaBr}_x\text{Cl}_{4-x}$ and the calculations of the intermolecular overlap integrals of the highest occupied molecular orbital of BETS were made to elucidate a key factor of the superconducting transition mechanism. The x dependence of intermolecular overlap integrals suggests that the magnitude of "spin gap" of non-magnetic insulating state tends to be diminished with decreasing x . There exists one intermolecular overlap integral exhibiting large temperature and x dependencies, which seems to play a crucial role in determining the nature of the ground state.

IV-G Structural Studies at Low Temperature and High Pressure

Since the molecular crystal is very soft and rich in the structural freedom, various structural phase transitions will be expected at high pressure and/or low temperature. Moreover, the electronic properties of molecular crystal are very sensitive to the structure change. Therefore the precise three-dimensional X-ray structure analyses at high pressure and/or low temperature are important in the studies on solid state properties of molecular crystals. More than several years ago we have developed X-ray imaging plate system equipped with liquid He refrigerator. Although some improvements are needed in the old type system, similar low-temperature X-ray systems become to be used in some laboratories in Japan.

As for the high pressure studies, we have made preliminary high-pressure diffraction experiments on two molecular conductors with triclinic unit cells by using beryllium cell and X-ray imaging plate system. The pressure dependence of the lattice constants and the crystal structures were determined. Although the quality of the collected X-ray reflection data were fairly good, the further improvement was needed to reduce the back ground reflections. Furthermore, the maximum pressure of the beryllium cell was too low (< 7 kbar). We are now examining a specially designed X-ray diamond anvil. A spectrometer was set up to determine the pressure by the shift of ruby fluorescence spectrum.



Spectrometer for monitoring the pressure of the diamond anvil cell

IV-G-1 High Pressure Structure of $[(\text{C}_2\text{H}_5)_2(\text{CH}_3)_2\text{N}][\text{Pd}(\text{dmit})_2]_2$

Takafumi ADACHI, Bakhyt NARYMBETOV, Hayao KOBAYASHI and Akiko KOBAYASHI (*Univ. Tokyo*)

As the first step of the crystal structure studies on molecular crystals at high pressure, we tried to analyze the crystal structure of high-pressure superconductor, $[(\text{CH}_3)_2(\text{C}_2\text{H}_5)_2\text{N}][\text{Pd}(\text{dmit})_2]_2$, which has an unusual phase diagram. Almost the same phase diagram was recently found in the similar $\text{Pd}(\text{dmit})_2$ superconductor by Kato et al. We have proposed a HOMO-LUMO inversion mechanism to explain the reason why the insulating phase appears when the superconducting phase is suppressed by pressure. Although the three-dimensional crystal structure analysis was successfully made around 5 kbar, the maximum pressure of our Be-cylinder type cell was insufficient to examine the HOMO-LUMO inversion mechanism because the pressure-induced insulating phase appears around 9 kbar. Recently we examined the diffraction pattern of $[(\text{CH}_3)_2(\text{C}_2\text{H}_5)_2\text{N}][\text{Pd}(\text{dmit})_2]_2$ by using specially designed diamond anvil cell and X-ray imaging plate system, which will enable us to make structure studies at higher pressure region. Unlike usual X-ray diamond anvil cell, the Be disk is not used to reduce the back ground diffraction. In the preliminary experiments, a small crystal ($0.3 \times 0.2 \times 0.04 \text{ mm}^3$) was used but we could obtain sufficiently fine diffraction patterns (Figure 1).

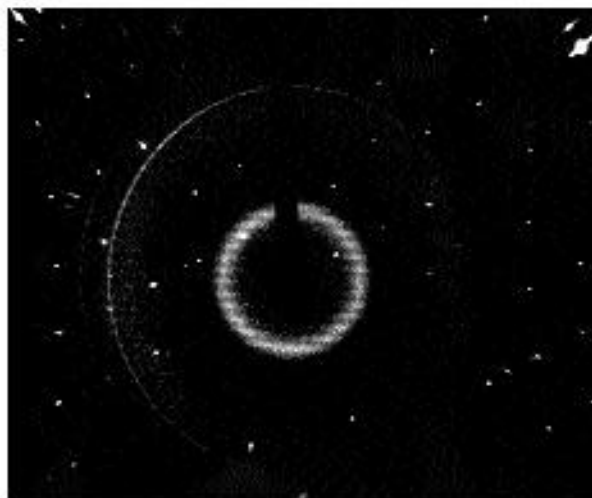


Figure 1. Diffraction pattern from the crystal of $[(\text{CH}_3)_2(\text{C}_2\text{H}_5)_2\text{N}][\text{Pd}(\text{dmit})_2]_2$

IV-G-2 Low-Temperature Structural Analysis of $-(\text{BETS})_2\text{Cu}_{5-x}\text{I}_6$

Bakhyt NARYMBETOV, Hayao KOBAYASHI, Akiko KOBAYASHI (*Univ. Tokyo*), Nataliya KUSHCH (*Institute of Chemical Physics in Chernogolovka, Russia*) and Eduard YAGUBSKII (*Institute of Chemical Physics in Chernogolovka, Russia*)

$-(\text{BETS})_2\text{Cu}_{5-x}\text{I}_6$ is a novel organic metal compound with two-dimensional polymeric anion network. The electrical conductivity of this salt at ambient pressure has metallic behavior down to 25-30K and then undergoes M-I transition which is completely suppressed by applying a pressure about 10 kbar. After release of pressure the salt reveals the metallic properties down to 1.3K. In order to examine an existence of structural changes at low temperature we have carried out X-ray diffraction analysis of the structure at temperature below MI transition region (Figure 1). Low-temperature diffraction patterns were detected by Weissenberg type X-Ray imaging plate at 15K. There is some statistic disorder of Cu atoms in anion network and at low-temperature a little redistribution of populations of Cu atom positions are observed. Detail analysis of the structure show that there is turning of the planes forming by I and Cu atoms relatively to the planes of BETS molecule for about 1.5° .

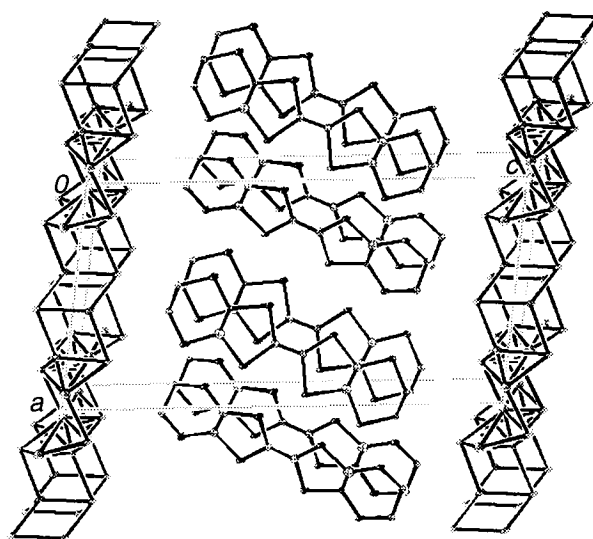
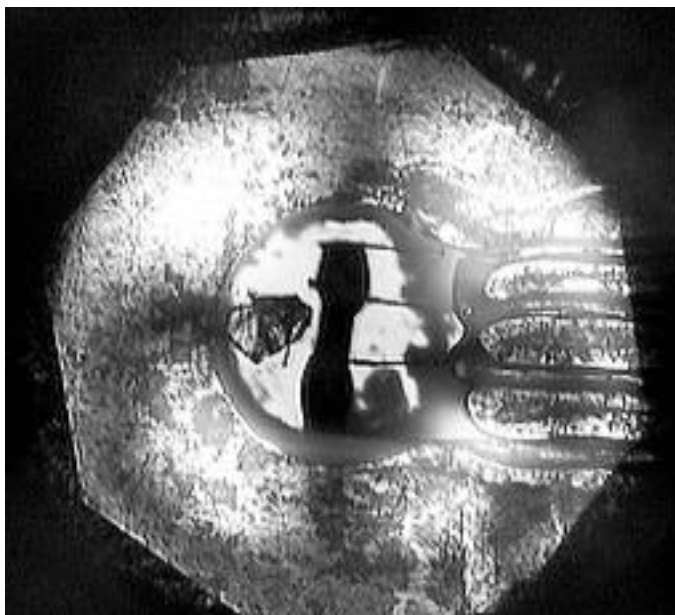


Figure 1. The crystal structure of $-(\text{BETS})_2\text{Cu}_{5-x}\text{I}_6$ at 15K.

IV-H Electrical Properties of Molecular Crystals at High Pressure

Pressure is one of the most important parameters in the studies of the physical properties of solids. Usually, the high-pressure resistivity measurements of molecular conductors have been made by using clamp type pressure cell up to about 20 kbar. The most convenient high-pressure apparatus at higher pressure region will be diamond anvil cell. However, despite of the pioneer work by Matsuzaki, the resistivity measurements by diamond anvil cell seems to have unsurmountable difficulties and there seems to be no report on the metallic systems. In the four-probe measurement, four leads bonded to the small fragile molecular crystal ($< 0.3 \text{ mm}$) must be took out through metal

gasket with keeping insulation. Although the technical difficulties seem to be very large, we have recently embarked on the high pressure resistivity experiments by using a conventional diamond anvil cell. The pressure was determined by the shift of fluorescence spectra of ruby crystals put in the gasket.



Crystal put in the gasket of the diamond anvil resistivity cell

IV-H-1 Pressure-Temperature Phase Diagram of $(\text{TMTTF})_2\text{PF}_6$

Takafumi ADACHI, Emiko OJIMA, Hayao KOBAYASHI and Takafumi MIYAZAKI (*Toyama Univ.*)

We have recently started to try the four-probe resistivity measurements on molecular conductors by using a conventional diamond anvil cell. Our present aim is to establish the technique for four-probe resistivity measurement up to about 50 kbar. As the first sample, we have selected $\text{TMTTF}_2\text{PF}_6$ system in view of the importance of the generalized phase diagram of Bechgaard salts proposed by Jerome et al. It has been believed that in TMTTF system with spin-Peierls (SP) ground state at ambient pressure, the ground state is changed as, SP → SDW (spin density wave) → SC (superconductor) with increasing pressure. $\text{TMTTF}_2\text{PF}_6$ is a good system to confirm these successive phase transitions. In order to examine the possibility of superconducting transition of this system, the resistivity measurements up to 40 kbar down to 0.5K will be required. Recently we have succeeded to measure the resistivity up to 45 kbar down to 2K and confirmed the suppression of the insulating phase. However much effort must be paid to overcome many difficulties in the experimental procedure.

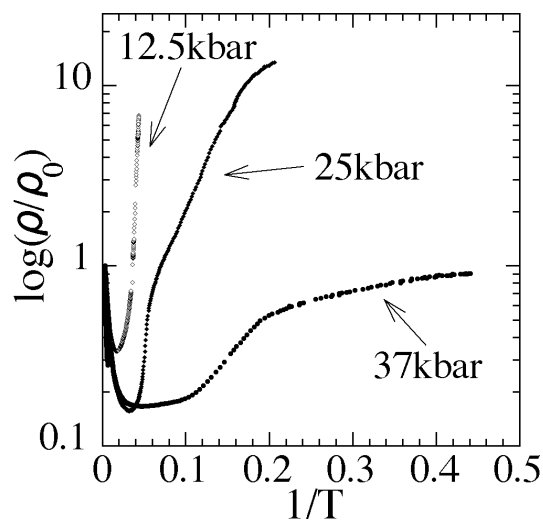


Figure 1. Pressure dependence of the resistivity behavior of $\text{TMTTF}_2\text{PF}_6$.

IV-I Development of New Molecular Conductors

The development of new materials is the most important driving force for the field of solid state chemistry. The recent progress of concept of the molecular design enriched greatly the physics and chemistry of crystalline molecular solids. The appearance of various types of molecular metals, superconductors and molecular

ferromagnets have attracted an increasing interest of chemists and physicists. We must grow out of the conventional design of molecular conductors for the future development. In these point of view we have performed the development of several types of new molecular components for organic molecular conductors. In the study of polythio-substituted TTF systems and ditellurium bridged polyacene donors we have determined the whole of the crystal structures and physical properties. We are now examining new guiding principles for designing the organic conductors. Furthermore we have developed the novel organic donor containing a stable organic radical part to investigate the interaction between itinerant electrons of the charge-transfer complexes and localized spins of the organic stable radical parts for the development of novel organic conducting-magnetic hybrid materials.

IV-I-1 Novel Stable Metallic Salts Based on a Donor Molecule Containing *Peri*-Ditellurium Bridges, TMTTeN

Emiko ARAI, Hideki FUJIWARA, Hayao KOBAYASHI, Akiko KOBAYASHI (*Univ. Tokyo*), Kazuo TAKIMIYA (*Hiroshima Univ.*), Tetsuo OTSUBO (*Hiroshima Univ.*) and Fumio OGURA (*Kinki Univ.*)

[*Inorg. Chem.* **37**, 2850 (1998)]

The first stable organic metals of the *peri*-ditellurium-bridged polyacene donor 2,3,6,7-tetramethylnaphtho[1,8-*cd*:4,5-*c'd'*]bis[1,2]ditellurole (TMTTeN) were obtained. In the crystal of TMTTeN₂-M(CN)₂ (M = Ag, Au), the donor molecules are stacked to form columns along *c*-axis of the tetragonal unit cell. They also develop three-dimensional network through the intermolecular Te...Te contacts. The salts are highly conductive (500-1000 S cm⁻¹) and keep the metallic states down to low temperature. Furthermore Ag(CN)₂ salt exhibited constant Pauli paramagnetic behavior down to 2K (para 2.0-2.5 × 10⁻⁴ emu/mol). The extended Hückel tight-binding band calculation gave the quasi-three dimensional Fermi surfaces owing to the three-dimensional Te...Te network and the tetragonal lattice symmetry. Crystal data for (TMTTeN)(CS₂): C₁₅H₁₂Te₄S₂, triclinic, *P*-1, *a* = 10.812(5), *b* = 14.588(6), *c* = 6.295(3) Å, α = 100.49(4), β = 106.75(4), γ = 89.90(4)°, *V* = 933.5(7) Å³, *Z* = 2. Crystal data for the Ag(CN)₂⁻ salt: TeAg_{0.12}C_{3.75}N_{0.25}H₃, tetragonal, *P*4₂/ncm, *a* = 18.2911(9), *c* = 5.352(1) Å, *V* = 1790.5(4) Å³, *Z* = 16. Crystal data for the Au(CN)₂⁻ salt: TeAu_{0.12}C_{3.75}N_{0.25}H₃, tetragonal, *P*4₂/ncm, *a* = 18.322(1), *c* = 5.350(3) Å, *V* = 1795.9(9) Å³, *Z* = 16.

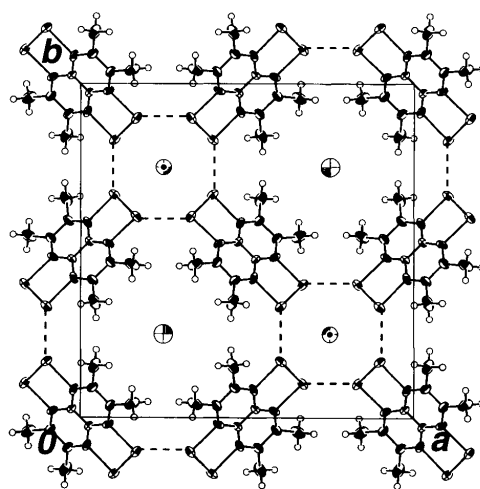
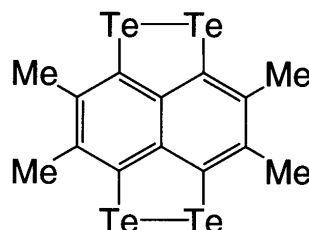


Figure 1. TMTTeN structure and crystal structure of its Au(CN)₂⁻ salt.

IV-I-2 Synthesis and Properties of a New Organic Donor Containing an Organic Radical Part: TEMPOET

Hideki FUJIWARA and Hayao KOBAYASHI

[*Synth. Met.* in press]

Recently the interplay between the conductivity and magnetism has been focused in the research of new organic conductors. Among them, several donors containing a stable organic radical part have been prepared to investigate the interaction between itinerant electrons of the charge-transfer complexes and localized spins of the organic stable radical parts for the development of novel organic conducting-magnetic hybrid materials. We report herein the synthesis and properties of a novel organic donor TEMPOET **1**. A novel electron donor TEMPOET was synthesized from the ketone derivative as air-stable orange microcrystals in 42% yield. The ESR spectrum of benzene solutions of TEMPOET and the ketone showed three absorption lines (*g* = 2.0061, *a_N* = 15.1 G) characteristic of the TEMPO radical and almost quantitative spin concentration. The static magnetic susceptibilities of the

ketone **3** and TEMPOET revealed that TEMPOET shows paramagnetic susceptibility corresponding to one spin per molecule and slightly antiferromagnetic interaction at low temperature region ($T = -1.00\text{K}$). On the other hand the ketone **3** indicated very weak ferromagnetic short-range interaction ($T = +0.55\text{K}$). TEMPOET shows one pair of reversible redox waves (0.88 V vs. Ag/AgCl) and three pairs of irreversible ones (+0.56, +1.17, +1.77V). The first oxidation potential, +0.56V, is almost the same as that of BEDT-TTF (+0.53 V), indicating its appropriate donating ability. Comparing its oxidation potentials to those of the corresponding tetramethylpiperidine analog (+0.55, +0.87 and +1.74 V), the oxidation of the TEMPO radical part seems to occur at the third oxidation process (+1.17 V), suggesting the possibility of the formation of its cation-radical salts with TEMPO radical part.

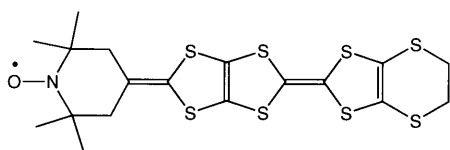


Figure 1. Structure of **1**.

IV-I-3 Synthesis, Structure and Physical Properties of Tetraalkylammonium Bis(5,6-dihydro-1,4-dithiin-2,3-diselenolato)-nickelate, $(R_4N)[Ni(dddS)_2]$ ($R = \text{Me, Et and } n\text{-Bu}$) and Neutral Complex $[Ni(dddS)_2]_2$

Hideki FUJIWARA, Emiko OJIMA, Hayao KOBAYASHI, Thierry COURCET (*LCC-CNRS*), Isabelle MALFANT (*LCC-CNRS*) and Patrick CASSOUX (*LCC-CNRS*)

[*Eur. J. Inorg. Chem.* in press]

Novel metal complexes $(R_4N)[Ni(dddS)_2]$ ($R = \text{Me, Et and } n\text{-Bu}$, $dddS = 5,6\text{-dihydro-1,4-dithiin-2,3-diselenolato}$) have been prepared and their crystal structures determined. The neutral $Ni(dddS)_2$ species was obtained by electrochemical oxidation from the monoanionic $(n\text{-Bu}_4N)[Ni(dddS)_2]$ complex. X-Ray crystal structure analyses of this neutral species show that two $Ni(dddS)_2$ are connected by the two Ni-Se bonds. Thus, the $Ni(dddS)_2$ entities form $[Ni(dddS)_2]_2$ dimers which are arranged face-to-face and rotated by about 90° with respect to each other (Figure 1). The electrochemical behavior of $(n\text{-Bu}_4N)[Ni(dddS)_2]$ indicates the possible formation of cation-radical species. The room temperature magnetic susceptibility measurements showed that the $(R_4N)[Ni(dddS)_2]$ complexes are paramagnetic with $\mu_{\text{eff}} = 1.77\text{-}1.83 \mu_B$, corresponding to one unpaired electron per molecular formula. The temperature dependence of the magnetic susceptibility of $(Et_4N)[Ni(dddS)_2]$ is indicative of weak long-range antiferromagnetic ordering below 9K. The dimerization in $[Ni(dddS)_2]_2$ results in a strong antiferromagnetic spin coupling within the dimer, and explain the non magnetic state observed for this compound.

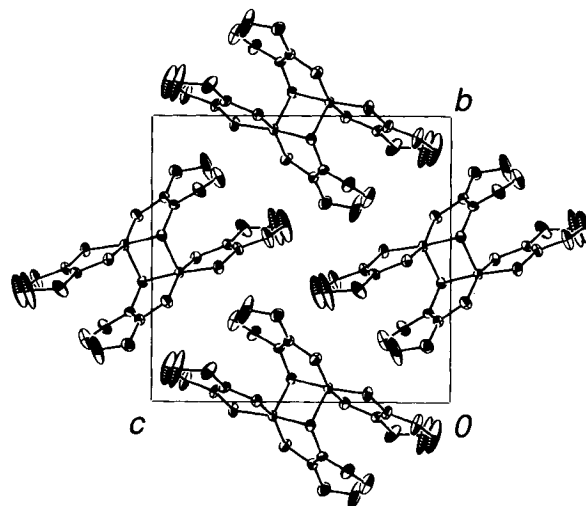


Figure 1. Crystal structure of neutral $[Ni(dddS)_2]_2$.

IV-I-4 Synthesis, Structure and Properties of a New Derivative of Sulfur-Bridged TTF Dimer

Hideki FUJIWARA, Emiko ARAI and Hayao KOBAYASHI

[*Synth. Met.* in press]

Synthesis of tetrathiafulvalenophane has been first reported in 1980 and extensively developed in 1990's because of its unusual molecular structure and interesting intramolecular interaction. We focused on a polysulfide chain as a bridging chain because it has more rigid framework than that of polymethylene chain and large interplanar interaction between two TTF moieties may be realized in a dimer. We report here the synthesis and structure of cyclopenteno-fused derivative of a novel cyclophane-like trisulfide-bridged TTF dimer **1** in which two TTF moieties are connected to each other by two trisulfide chains. New derivative **1** was synthesized by the same procedures of the tetrakis-(methylthio) derivative. Preparation of cation radical salts was performed by electrochemical oxidation in chlorobenzene. The composition of the PF_6^- salt of **1** is 1:1 (Donor:Anion) and donors are in the monocationic state, in other words, each TTF moieties are in the semication state. The TTF moieties have planar structure and eclipse almost perfectly to each other with comparatively short interplanar distance of 3.65 Å. Each dimers are stacked each other and formed one-dimensional columnar donor arrays of the dimer molecules along a -axis. This salt shows semiconducting behavior with comparatively high conductivity of $\sigma_{\text{rt}} = 10^{-1} \text{Scm}^{-1}$.

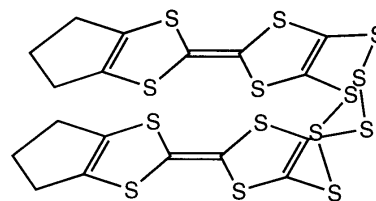


Figure 1. Structure of **1**.

IV-I-5 Synthesis, Structures and Properties of an Unsymmetrical Donor Containing Pyradino-Ring (PEDTTSeF) and Its Cation Radical Salts

Emiko OJIMA, Hideki FUJIWARA and Hayao KOBAYASHI

In the design of new molecular conducting systems, it is expected to enhance the intermolecular interaction by the condensation of hetero ring and/or the substitution of chalcogen atoms. In recent years the diazino-, pyrizino-, pyrazino- and dimethylpyrazino-condensed tetrathiafulvalenes have received attention as the materials for realization of two- or three-dimensional conducting property through the S-S or S-N intermolecular contacts. From this viewpoint, we have synthesized a novel unsymmetrical donor containing pyradino-ring: PEDTTSeF. The crystal structure and electrochemical property of the neutral molecule have been investigated. The CV result indicates that the donor molecule shows two pairs of reversible redox waves (+0.85 and 1.18 V vs. Ag/AgCl in PhCN) and its electron-donating ability is lower than that of BETS by the condensation of pyradino-ring. Furthermore we prepared several cation radical salts of this new donor by electrochemical oxidation. The temperature dependence of the electrical resistivities of the BF_4^- , ClO_4^- , GaCl_4^- , PF_6^- and AsF_6^- salts are metallic down to low temperature and several of which show metal-insulator transition. The crystal structure analyses of the BF_4^- and ClO_4^- salts reveal that these salts have 2:1 composition of D:A and are isomorphous to each other. There are many short intermolecular contacts and two-dimensional networks through the hetero atoms (Figure 1). The magnetic susceptibility of the BF_4^- salt was measured by SQUID magnetometer down to 2K. The paramagnetic susceptibility is almost constant throughout the temperature range, indicating the Pauli paramagnetism of the metal electrons (*ca.* 5.0×10^{-4} emu/mol).

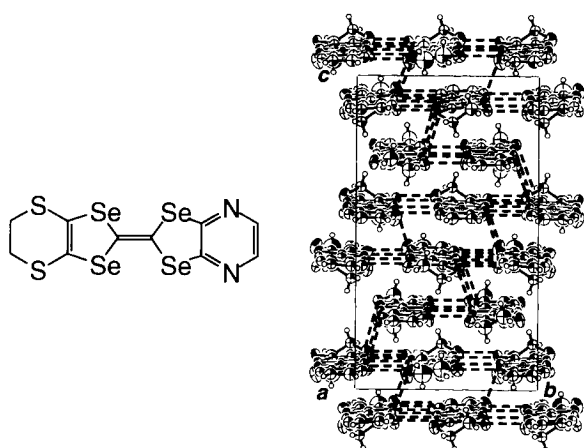


Figure 1. PEDTTSeF structure and donor arrangement of its BF_4^- salt.

IV-I-6 Development of Novel Organic Conductors Based on Tellurium Containing Donor Molecules

Emiko OJIMA, Hideki FUJIWARA, Bakhyt NARYMBETOV, Hayao KOBAYASHI and Akiko KOBAYASHI (*Univ. Tokyo*)

In the search for superior electron donors for organic conductor, the tellurium-containing TTF derivatives have drawn much attention, because the introduced tellurium atoms are expected to produce a novel metallic system in which wide bandwidth and high dimensionality may be realized due to the large van der Waals radii and electron density of tellurium atoms. Furthermore conducting salts based on tellurium-containing donor molecules are interesting because the tellurium network in the crystal is dominant for the construction of whole the crystal structure. Because of their low solubility to organic solvents and difficulty of synthesis, however, the systems based on tellurium-containing donor molecules have not received much attention compared to the systems based on sulfur- or selenium-containing donors as yet. Therefore we focused on the development of new tellurium-containing donors and prepared new trimethyleneditelluro- and trimethyleneoxaditelluro-substituted dimethyl-TTF derivatives. The electrochemical properties of the neutral molecules have been investigated. The CV result indicates that trimethyleneditelluro-substituted dimethyl-TTF derivative shows peculiar multi-redox behavior, though trimethyleneoxaditelluro-substituted dimethyl TTF derivative shows conventional two pairs of reversible redox waves. Preparation of the conducting salts and their physical property measurements are now in progress.

IV-J Development of Pulsed Field Gradient NMR Spectroscopy

Pulsed field gradient spin echo (PGSE) nuclear magnetic resonance (NMR) is a powerful method for the study of dynamics in condensed matter since it probes translational motion of molecules selectively, without being affected by vibrational or rotational motions. Due to this advantage it has been widely applied to the dynamics of molecules in liquids. However, applications of this technique to strongly dipole-coupled spin systems with short T₂ or to the study of slow and anisotropic self-diffusion are still challenging works because combined techniques of line-narrowing, pulsing of sharp and intense field gradients, and two-dimensional field-gradient generation are necessary.

In the present study we applied the technique to the study of anisotropic self-diffusion in liquid crystals and also to the diffusion of lithium ions in sulfide glasses, with the use of the laboratory-made spectrometer equipped with a rotatable quadrupole gradient coil.

IV-J-1 Inversion of Self-Diffusion Anisotropy within a Smectic A Phase of Liquid Crystal

Osamu OISHI and Seichi MIYAJIMA

A technique of PGSE-NMR coupled with a quadrupole coil rotation¹⁾ was applied to the study of self-diffusion anisotropy in a liquid crystalline material OBBF, 4-(4-octyloxybenzoyloxy)benzylidene(4-fluoro)aniline. It was found, as shown in Figure 1, that the self-diffusion anisotropy was inverted within a smectic A (S_A) phase: The diffusion coefficient component perpendicular to the director, D_{\perp} , is larger than the component parallel to the director, D_{\parallel} (which means the diffusion within the layer is faster than that across the layer) in the low temperature region of the S_A phase, but the anisotropy was inverted in the high temperature region. The two activation energies were significantly different, namely, 31 kJ mol⁻¹ for D_{\perp} , and 55 kJ mol⁻¹ for D_{\parallel} .

Reference

- 1) O. Oishi and S. Miyajima, *J. Magn. Reson. Ser. A*, 123, 64 (1996).

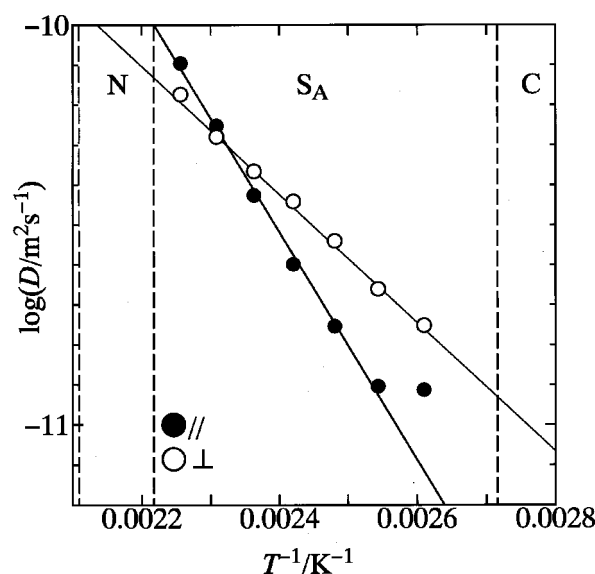


Figure 1. Components of the self-diffusion coefficient tensors, D_{\parallel} (parallel to the director) and D_{\perp} (perpendicular to the director), in S_A phase of OBBF.

IV-J-2 Ion Dynamics in Superionic Glasses by ⁷Li NMR

Tomoko AKAI (*Osaka Natl. Res. Inst.*), Osamu OISHI and Seichi MIYAJIMA

[*Solid State Commun.* submitted]

Dynamics of lithium ions in superionic glasses have been investigated by ⁷Li NMR. In the study of ionic transport mechanism, it is important to evaluate the rate of ionic hopping in the short-range and long-range transport independently because the ionic conduction is a result of correlated microscopic motions of individual ions. For this purpose, we measured spin relaxation rate and diffusion coefficient. Hopping rate of the ions was determined from the temperature dependence of spin relaxation rate. The diffusion coefficient was measured in a compound 0.7Li₂S-0.3B₂S₃ by a pulsed field gradient spin echo (PGSE) method. From these data, it was suggested that considerable portion of ions move backward after the initial hoppings.

IV-K Phase Transitions and Dynamical Ordering in Liquid Crystals

Extensive high resolution NMR studies were conducted to reveal the microscopic origins of antiferroelectricity and reentrant phase transitions in liquid crystals. ^{13}C and ^2H NMR revealed interesting features of the antiferroelectric liquid crystalline material, especially on aspects of freezing of conformational motion and asymmetric hindrance of the chiral chain motion. Neutron diffraction study was also started for reentrant liquid crystals.

IV-K-1 Complete Assignment of ^{13}C NMR Spectra and Determination of Orientational Order Parameter for Antiferroelectric Liquid Crystal MHPOBC

Toshihito NAKAI (*Univ. Tsukuba and IMS*), Hiroki FUJIMORI (*Nihon Univ. and IMS*), Daisuke KUWAHARA and Seichi MIYAJIMA

[*J. Phys. Chem. B* submitted]

Complete assignment of the ^{13}C NMR lines was accomplished for both isotropic and oriented samples of antiferroelectric liquid crystal MHPOBC (Figure 1). Two-dimensional double-quantum coherence spectroscopy (2-D INADEQUATE) in the isotropic phase, and field alignment-induced shifts (AIS) were studied. ^{19}F - ^{13}C dipolar quartets were measured for TFMHPOBC, where a methyl group attached to the chiral center of MHPOBC is replaced by a trifluoromethyl group, to assist the assignment. Shielding tensor principal elements were determined for each carbon by site-separated spinning sideband spectroscopy (2-D TOSS-deTOSS). The orientational order parameter has been evaluated to be 0.73 at 403 K in S_A phase, by using the experimentally determined AIS and the tensor elements and by assuming an intramolecular free rotation model.

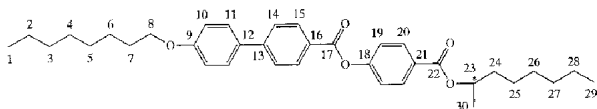


Figure 1. MHPOBC with the numbering scheme for the carbon atoms.

IV-K-2 Freezing of Intramolecular Motion around the Chiral Center of Antiferroelectric Liquid Crystal as Evidenced by Transient Oscillation in ^{13}C - ^1H Cross Polarization Dynamics

Hiroki FUJIMORI (*Nihon Univ. and IMS*), Jean-Pierre BAYLE (*Univ. Paris XI and IMS*) and Seichi MIYAJIMA

[*Chem. Phys. Lett.* submitted]

Transient coherent effect is observed in the process of ^{13}C - ^1H cross polarization when individual ^{13}C spins are dipole-coupled to a small number of protons and the spin-diffusion rate of ^1H is low enough. In this study we opened a new application of this transient effect to the

analysis of intramolecular motion in liquid crystal. Decay time of oscillation, which is determined by ^1H spin-diffusion, probes how the intramolecular ^{13}C - ^1H dipole interactions are averaged out, and hence detects the change of intramolecular motion. Figure 1 shows the oscillations observed for the aromatic protonated carbons of MHPOBC in the paraelectric smectic A (S_A) phase ((a) and (b)) and in the antiferroelectric smectic CA^* (S_{CA^*}) phase ((c) and (d)). It was shown that chain conformational motions around the chiral center are different in the two phases: A large amplitude motion in S_A is frozen to a significant extent in S_{CA^*} , and hence enables a large transverse dipole moment of a molecule to come out.

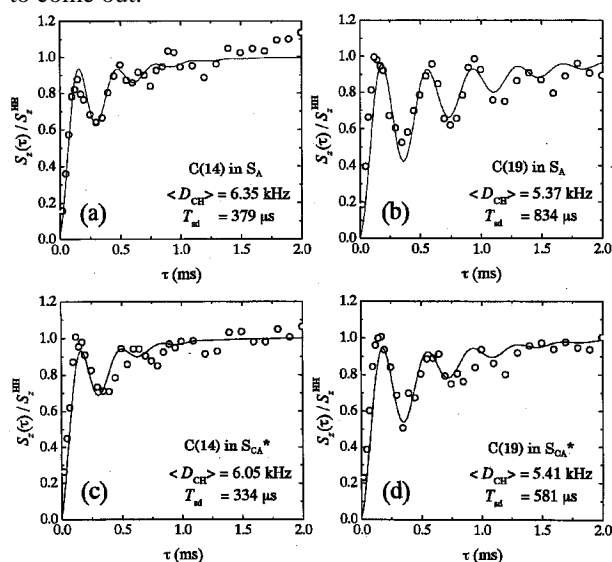


Figure 1. Time evolution of ^{13}C magnetizations of C(14) and C(19) during the ^{13}C - ^1H double resonance in the rotating reference frame for MHPOBC. See Figure 1 of IV-b-1 for the carbon site numbers.

IV-K-3 Transient ^{13}C - ^1H Nuclear Overhauser Effect in Liquid Crystal

Hiroki FUJIMORI (*Nihon Univ. and IMS*), Daisuke KUWAHARA, Toshihito NAKAI (*Univ. Tsukuba and IMS*) and Seichi MIYAJIMA

[*J. Magn. Reson.* submitted]

Significant transient ^{13}C - ^1H nuclear Overhauser effect (NOE) was observed in liquid crystal, and was explained quantitatively by a local ^{13}C - ^1H dipole interaction. Figure 1 shows three different pulse sequences used for the present experiment and the observed ^{13}C magnetization recoveries. The recovery

after the Hartman-Hahn signal enhancement (B) deviated significantly from the exponential behavior. Remarkably large maximum amounting to 2.5 times the equilibrium magnetization appeared in the Solomon's two-pulse sequence (C), and provided an interesting way of estimating the transition probabilities between the coupled spin states. Experimental data are obtained for an antiferroelectric chiral smectic liquid crystal MHPOBC.

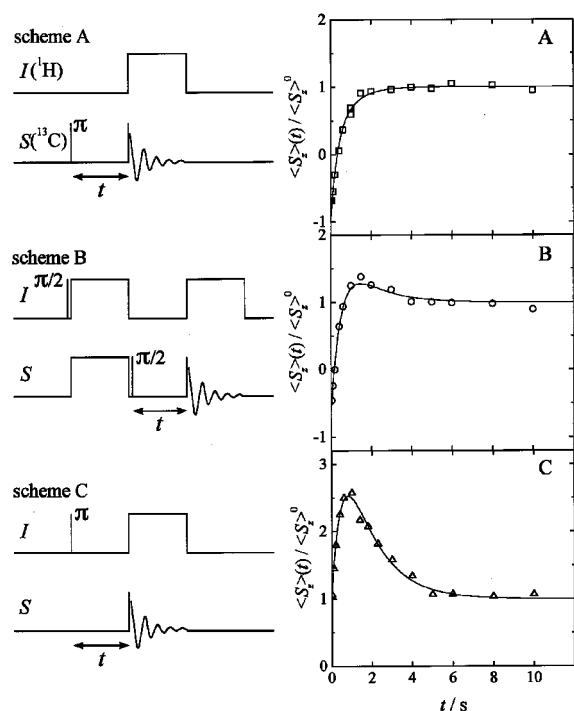


Figure 1. Three pulse sequences and the respective time-evolutions of ^{13}C magnetizations measured at C(19) for MHPOBC in S_A phase. The solid curves are drawn on the basis of coupled master equations for a dipole-coupled ^{13}C - ^1H spin pair.

IV-K-4 Asymmetrical Hindrance of Methylene Group Rotations about the Chiral Alkyl Chain Axis in the Smectic A Phase of an Antiferroelectric Liquid Crystal as Observed by ^2H -NMR

Shohei YOSHIDA (Tokyo Inst. Tech.), Bo JIN (Tokyo Inst. Tech.), Koh TOKUMARU (Tokyo Inst. Tech.), Yoichi TAKANISHI (Tokyo Inst. Tech.), Ken ISHIKAWA (Tokyo Inst. Tech.), Hideo TAKEZOE (Tokyo Inst. Tech.), Atsuo FUKUDA (Shinshu Univ.), Tetsuo KUSUMOTO (Sagami Cent. Res. Center), Toshihito NAKAI (Univ. Tsukuba) and Seiichi MIYAJIMA

[Phys. Rev. E submitted]

A number of homologues of MHPOBC with selectively deuterated methylenes were synthesized, and the ^2H -NMR spectra were detected. The quadrupolar splitting widths of methylenes in the chiral chain are about one-third of those in the achiral chain, and this result gives a clear evidence of the bent chiral chain. A most striking fact is that the chiral chain methylenes exhibited anomalously large double splittings,

indicating that the two deuterons belonging to one methylene unit are not equivalent. This gives an evidence of extremely asymmetric rotational potentials of the methylenes near the chiral center.

IV-K-5 Molecular Rotation in Antiferroelectric Liquid Crystal Studied by ^{13}C -NMR Spin-Lattice Relaxation Time Measurement

Koh TOKUMARU (Tokyo Inst. Tech.), Bo JIN (Tokyo Inst. Tech.), Shohei YOSHIDA (Tokyo Inst. Tech.), Yoichi TAKANISHI (Tokyo Inst. Tech.), Ken ISHIKAWA (Tokyo Inst. Tech.), Hideo TAKEZOE (Tokyo Inst. Tech.), Atsuo FUKUDA (Shinshu Univ.), Toshihito NAKAI (Univ. Tsukuba) and Seiichi MIYAJIMA

[Jpn. J. Appl. Phys. submitted]

Temperature dependence of the spin-lattice relaxation time T_1 was measured in an antiferroelectric liquid crystal MHPOBC by means of ^{13}C NMR. The activation energies determined by the temperature dependences of T_1 are the same for most of the carbon nuclei in the S_A and S_{CA}^* phases, whereas they are different for carbon nuclei at the chiral center and at the carbonyl carbons. The overall molecular rotation about its long axis does not change through the phase change from S_A to S_{CA}^* . Critical slowing down of this rotational motion was not observed.

IV-K-6 Neutron Diffraction Study of a Reentrant Liquid Crystal

Osamu OISHI, Seiichi MIYAJIMA, Michihiko NAGAO (Univ. Tokyo) and Masayuki IMAI (Univ. Tokyo)

When conventional liquid loses its isotropic (I) symmetry and assumes uniaxial orientational order, the nematic (N) liquid crystalline state is formed. The smectic A (S_A) state is characterized by its one-dimensional translational order in addition to the nematic order. It is therefore natural that the phase transition sequence be I-N- S_A on lowering the temperature. However, the present compound, CBOBP (4-cyanobenzoyl-oxy-[4-octyl-benzoyloxy]-*p*-phenylene), exhibits a transition sequence, I-N- S_{Ad} -N- S_{A1} (doubly reentrant sequence) on lowering the temperature. The second N phase is called reentrant nematic (RN), and the S_{Ad} to RN transition means that 1-D translational lattice *melts* on lowering the temperature. Due to this peculiarity, the nature of this transition sequence has been one of the interesting topics in recent liquid crystal research.¹⁾

We made neutron diffraction study to clarify the structure of the liquid crystalline phases and hence to clarify the microscopic mechanism of this phenomenon. For this purpose a compound with perdeuterated chain, CBOBP- d_{17} was prepared. Small angle neutron diffraction instrument (SANS-U) of JAERI at Tokai was used at a wavelength of 7.0 Å with a velocity selector.

Figure 1 shows the intensity of the smectic primary

peak. What is striking is that the peak intensity was very small in S_{Ad} phase; smaller than those in N or RN phases, and therefore the reentrant *melting* seems to accompany *increase* in peak intensity. This revealed highly disordered chain structure in the S_{Ad} mesophase, in accordance with the deuterium NMR study.¹⁾

Reference

1) S. Miyajima and T. Hosokawa, *Phys. Rev. B* **52**, 4060 (1995).

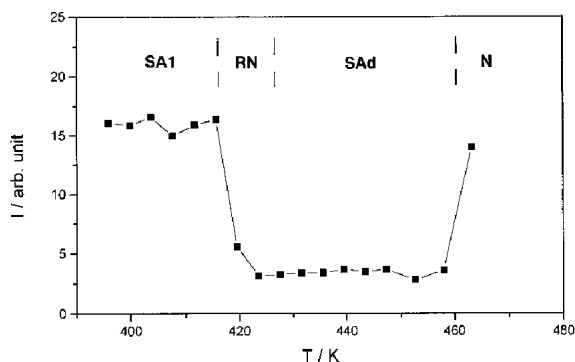


Figure 1. Temperature dependence of the diffraction intensity of the smectic primary peak for CBOBP-*d*17.

IV-K-7 ^{13}C NMR Study of a Reentrant Liquid Crystal

Hiroki FUJIMORI (*Nihon Univ. and IMS*), Daisuke KUWAHARA and Seiichi MIYAJIMA

^{13}C NMR experiments were carried out for a

reentrant liquid crystal CBOBP, 4-cyanobenzoyloxy-[4-octylbenzoyloxy]-*p*-phenylene, and its chain-deuterated analogue, CBOBP-*d*17. Temperature dependences of the alignment-induced shift and the transient behavior in ^{13}C - ^1H cross-polarization dynamics were analyzed for oriented samples. It was shown, as in Figure 1, that chemical shifts for aromatic protonated carbons exhibited anomalous increase in S_{A1} phase. Transient oscillation frequency, $\langle D_{\text{CH}} \rangle$, exhibited similar behavior showing that $\langle D_{\text{CH}} \rangle$ is determined predominantly by the orientational order parameter, but the increase in S_{A1} phase is less clear.

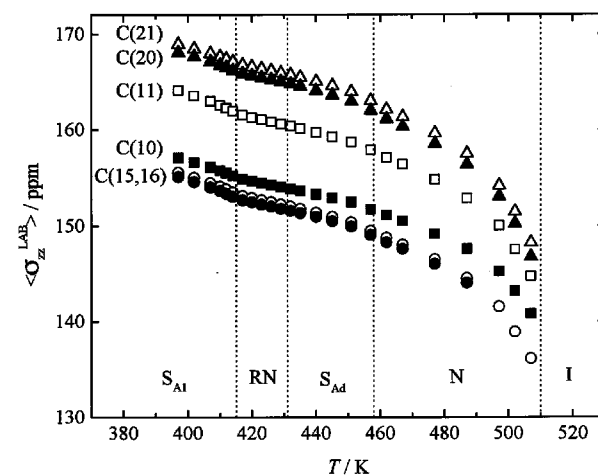


Figure 1. Temperature dependence of the ^{13}C NMR absorption position (measured from tetramethylsilane) for the aromatic protonated carbons of CBOBP.

IV-L Electronic Properties of Alkali-Hydrogen-Carbon Systems

In alkali-hydrogen-carbon ternary systems, hydrogen or alkali metal elements exhibit a variety of electronic states when doped or intercalated in the host crystal lattice. An interesting feature is how the hydrogen $1s$ state contribute to the bulk electronic properties. Structural and electronic properties were studied for sodium-hydrogen-graphite ternary compound by means of the first principle local density functional calculation of the electronic state and the electric field gradient at sodium site. Local electronic state at hydrogen atom was investigated in sodium-hydrogen- C_{60} ternary superconductor by ^1H NMR spin lattice relaxation time measurement. The effect of hydrogen absorption on the structural and electronic properties in K_3C_{60} superconductor was investigated by means of powder X-ray diffraction, magnetic susceptibility measurement, and solid state NMR spectroscopy. An attempt at detecting and controlling the reaction of potassium hydride with C_{60} crystal was conducted with *in-situ* ^1H NMR measurements. New alkali-hydrogen- C_{60} compounds were synthesized and characterized by powder X-ray diffraction and solid state NMR measurements.

IV-L-1 First-Principles Study on Structure and Electronic State of NaH-Graphite Ternary Intercalation Compound

Shin'ichi HIGAI (*Univ. Tsukuba*), Toyoki FUJIWARA (*Univ. Tsukuba*), Shugo SUZUKI (*Univ. Tsukuba*), Kenji NAKAO (*Univ. Tsukuba*), Seiji MIZUNO (*Hokkaido Univ.*), Hironori OGATA and Seiichi MIYAJIMA

The structure and electronic state of NaH-graphite ternary intercalation compound have been theoretically studied based on the first-principles calculation. In

order to make clear the structure of intercalated Na and H, we constructed a number of simple structural models, and calculated the total energy and the nuclear quadrupole coupling constant and asymmetry parameter of ^{23}Na . The structural model in which H exists as the H_2 molecule was found most stable, and could explain the result of ^{23}Na NMR spectroscopy. In the electronic band structure for this model, two kinds of bands form the metallic conduction states. One is the antibonding π -band of graphite, and another is the band which is composed of the antibonding $1s$ orbital of H_2 and the $3s$ orbital of Na. A part of the present calculation was performed with the IMS super computer system.

IV-L-2 ^1H NMR Study in $\text{Na}_4\text{HC}_{60}$ Superconductor

Hironori OGATA, Seiichi MIYAJIMA, Kenichi IMAEDA and Hiroo INOKUCHI

The local electronic state at hydrogen atom for the $\text{Na}_4\text{HC}_{60}$ superconductor has been investigated by spin-lattice relaxation time measurement of ^1H NMR. Figure 1 shows the temperature dependence of spin-lattice relaxation time (T_1) measured by the saturation recovery method at 60 MHz. No frequency dependence was observed for the value of T_1 among 60, 300 and 400 MHz in the temperature region between 120K and 340K. Below about 150K, the T_1 shows Korringa-like temperature dependence ($T_1 \times T = 740 \text{ s K}$) within experimental accuracy. This suggests that H $1s$ orbital contribute to the electronic state on the Fermi level. At about 260 K, a jump of T_1 is observed, which is caused by the increase of the density of states at Fermi level, $N(E_F)_{\text{Hatom}}$, above this temperature by the first order phase transition.

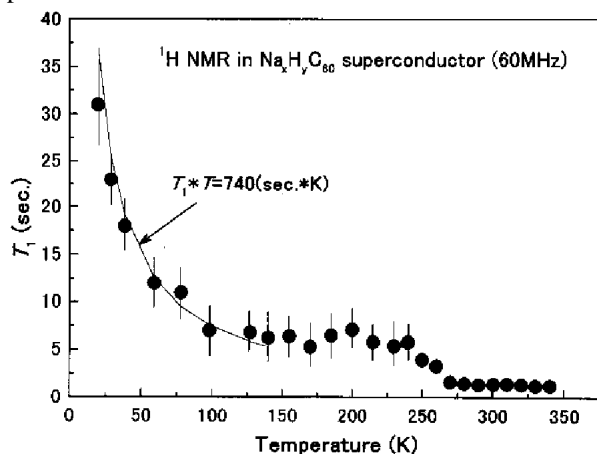


Figure 1. Temperature dependence of ^1H T_1 in $\text{Na}_4\text{HC}_{60}$ superconductor.

IV-L-3 Structural and Electronic Properties of Hydrogen-Absorbed Alkali- C_{60} Compounds

Hironori OGATA and Seiichi MIYAJIMA

[*Synthetic Metals* in press]

The effect of hydrogen absorption on the structural and electronic properties of single phase K_3C_{60} superconductor was investigated by means of powder X-ray diffraction, magnetic susceptibility measurement, and solid state NMR spectroscopy. No lattice expansion as well as no structural change were observed in powder X-ray diffraction by hydrogen absorption. Superconductivity was preserved, and the superconducting transition temperature did not change by hydrogen absorption. No distinct relationship is observed between the shielding fraction and the amount of absorbed hydrogen. Peak position and line shape of ^{13}C NMR spectrum did not change by hydrogen absorption. Peak position of ^1H NMR spectrum suggests that hydrogen is neutral in the crystal. No significant difference was observed between K_3C_{60} and hydrogen-absorbed

sample in ^{23}Na NMR spectra down to 200 K. This fact suggest that absorbed hydrogen does not occupy octahedral- or tetrahedral-site in the f.c.c. lattice. Curie-like behavior was observed in the temperature dependence of the intensity of ^1H NMR spectra. A possible explanation for the above experimental results would be that hydrogen reacts with C_{60} molecule on the surface of crystal grain, while the bulk samples of K_3C_{60} are free from hydrogenation for the hydrogen contents of 0.56.

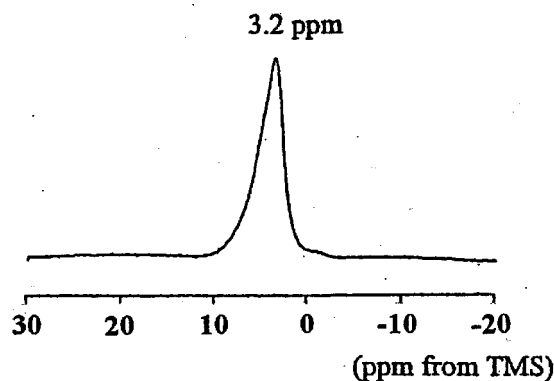


Figure 1. ^1H NMR spectrum of $\text{K}_3\text{C}_{60}\text{H}_{0.56}$ at room temperature.

IV-L-4 *In-Situ* NMR Study of the Reaction Process in Alkali-Hydrogen- C_{60} Compounds

Hironori OGATA and Seiichi MIYAJIMA

An attempt at detecting and controlling the reaction process of potassium hydride with C_{60} is reported. A mixture of stoichiometric amounts of potassium hydride and C_{60} powder was evacuated and sealed in a Pyrex tube, and heated in the NMR probe in several conditions. These reaction processes were monitored by *in-situ* ^1H NMR measurements. Figure 1 shows the time dependence of ^1H NMR spectra for the sample reacted at 457 K. After eight hours' reaction, a signal at about -6 ppm appeared, which may be ascribable to decomposed hydride ions. Just after the intensity of this peak became maximum, the sample was cooled rapidly to room temperature to stop the reaction. After cooling, the hydrogen peak exhibited down-field shift, showing the change of the hydrogen states from anionic toward neutral side. Powder X-ray diffraction profile of the final product showed that crystal structure of this sample was K_3C_{60} . Furthermore, the superconducting transition temperature was 19.4 K, same as that of K_3C_{60} .

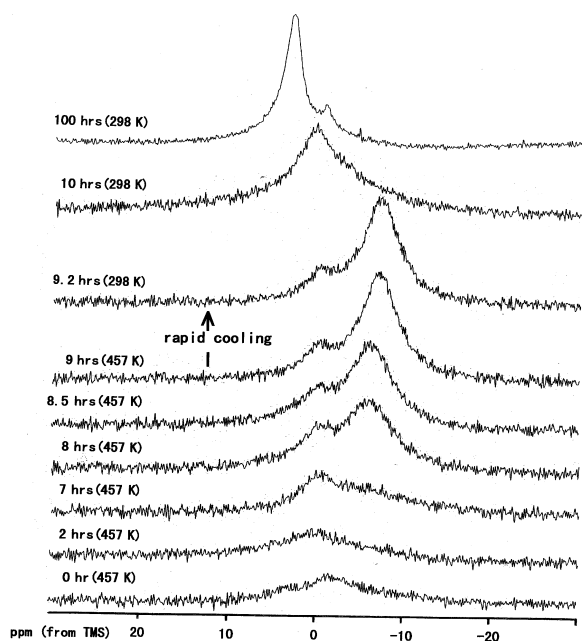


Figure 1. Time dependence of *in-situ* ^1H NMR spectra in the mixture of potassium hydride and C_{60} powder.

IV-L-5 Synthesis and Structural Study of New Alkali-Hydrogen- C_{60} Compounds

Hironori OGATA and Seiichi MIYAJIMA

$\text{Li}_x\text{H}_y\text{C}_{60}$, $\text{Na}_x\text{Li}_y\text{H}_z\text{C}_{60}$ and $\text{K}_x\text{Li}_y\text{H}_z\text{C}_{60}$ compounds were synthesized by the reaction of alkali metals, alkali hydrides and C_{60} solid, and characterized by powder X-ray diffraction and ^1H NMR. Powder X-ray diffraction profiles of these compounds showed that these crystals form single phase f.c.c. lattice. ^1H NMR spectra of these compounds suggest that hydrogen is in an anionic state in the crystal lattice.

IV-M Magnetic Local Structure and Magnetic Interactions in Molecule Based and Organic-Inorganic Hybrid Magnets

Organic ferromagnet is one of the realizations of great possibilities of organic molecules which can be designed to exhibit a variety of functions by chemical modifications and attracts interest of chemists in broad areas such as organic, physical, and theoretical chemistry, *etc.* Ferromagnetism of organic materials is of current interest. It is desired to clarify the mechanism of intermolecular magnetic interaction in a microscopic viewpoint to establish a leading principle to produce the ferromagnetic ordering in the crystalline phase of molecule based materials and to understanding the characters and the functions of open-cell molecules. Solid state high resolution NMR techniques provide an unique information of the magnetic local structure and the magnetic interactions in a microscopic view point. We have investigated the magnetic local structure and magnetic interaction for a variety of magnetic materials.

IV-M-1 Solid State ^1H -MAS-NMR and Spin Densities on Protons of the Organic Ferromagnetic Tempo Derivatives

Goro MARUTA (*Osaka Univ.*), Sadamu TAKEDA (*Gunma Univ. and IMS*), Takashi KAWAKAMI (*Osaka Univ.*), Wasuke MORI (*Kanagawa Univ.*), Ron IMACHI (*Univ. Electro-Commun.*), Takayuki ISHIDA (*Univ. Electro-Commun.*), Takashi NOGAMI (*Univ. Electro-Commun.*) and Kizashi YAMAGUCHI (*Osaka Univ.*)

[*Mol. Cryst. Liq. Cryst.* **306**, 307 (1997)]

Ferromagnetism in purely organic materials attracts a grate interest, since Kinoshita et al. reported a molecular ferromagnet at low temperature. Most examples of organic ferromagnetic crystals are based on nitroxide (N-O) radicals. Main interest of this field is to control the intermolecular magnetic interaction between N-O radical groups in the crystalline state to produce the ferromagnetic ordering. As a possible intermolecular ferromagnetic interaction path, a close contact of methyl and/or methylene protons to N-O radical group of adjacent molecules in crystal has been proposed from X-ray diffraction experiment. The

methyl and methylene protons are expected to be intermolecular ferromagnetic exchange coupler via spin polarization mechanism ($\text{NO}(\uparrow)\text{-C}(\uparrow)\text{-C}(\uparrow)\text{-H}(\uparrow)\cdots\text{NO}(\uparrow)$). The electron spin polarized on the proton is a key point. Electron spin densities on hydrogen atoms of 4-(arylmethyleneamino)-2,2,6,6-tetramethylpiperidin-1-oxyls (abbreviated as Ar-CH=N-TEMPO), which show ferromagnetic behavior at low temperatures, were determined in their crystalline phases from the temperature dependence of the Fermi contact shift measured by high speed magic angle spinning proton nuclear magnetic resonance. This method revealed a large negative hyperfine coupling constant for the methyl and methylene protons, $A = -1.0$ MHz for Ar = *p*-Cl-ph and $A = -1.3$ MHz for Ar = ph, and very small one for the aryl group protons, $|A| < 0.01$ MHz for *p*-Cl-ph and $A = +0.1$ MHz for ph. The observed negative hyperfine coupling constant (negative spin density) of methyl and methylene protons matches with spin alternation for the intermolecular spin polarization mechanism through the contact of methyl and/or methylene protons to adjacent N-O radical group. This contact potentially contributes to the intermolecular ferromagnetic interaction.

IV-M-2 Solid State High Resolution NMR

Studies of Electron Spin Densities in Charge-Transfer Complex-Based Organic Ferromagnets

Goro MARUTA (*Osaka Univ.*), **Sadamu TAKEDA** (*Gunma Univ. and IMS*), **Kizashi YAMAGUCHI** (*Osaka Univ.*), **Kazumasa UEDA** (*Osaka Pref. Univ.*) and **Toyonari SUGIMOTO** (*Osaka Pref. Univ.*)

[*Synth. Metals* submitted]

A variety of purely organic ferromagnets which consist of stable neutral radical species have been developed. Charge-transfer complex-based organic ferromagnets are particularly of current interest because of their potential to exhibit ferromagnetism at high temperatures. In these compounds, donor (D^+) and acceptor (A^-) can be designed to bear electron spins and electronic conduction can be also expected, so that the magnetic interaction in these salts may be different from those in neutral radical-based magnetic crystals and a novel magnetism is expected. A series of 4,4,5,5-tetramethylimidazolin-1-oxyls with 4-(*N*-R-pyridinium) groups at the 2-position ($1^{+\cdot}$: R = methyl, $2^{+\cdot}$: R = ethyl, $3^{+\cdot}$: R = *n*-propyl) form stable charge transfer complexes with the radical anion of TCNQF₄. It has been revealed by the magnetic susceptibility measurements that $1^{+\cdot}$ ·TCNQF₄^{-·} and $3^{+\cdot}$ ·TCNQF₄^{-·} are ferromagnets at low temperature ($T_c \sim 0.5$ K), whereas $2^{+\cdot}$ ·TCNQF₄^{-·} exhibits antiferromagnetic behavior. It is interesting to study the mechanism of magnetic interaction of these CT complexes. The mechanism can be elucidated from the electron spin density distribution in the magnetic crystals. In this work, we have determined the electron spin density distribution and the magnetic local structure in the salts of $1^{+\cdot}$ ·TCNQF₄^{-·}, $2^{+\cdot}$ ·TCNQF₄^{-·} and $3^{+\cdot}$ ·TCNQF₄^{-·} by solid state high resolution ¹H, ¹³C and ¹⁹F-NMR.

IV-M-3 Magic Angle Spinning ¹H-NMR Study of the Spin Density Distribution of Pyridyl Nitronyl Nitroxides in the Crystalline Phase

Goro MARUTA (*Osaka Univ.*), **Sadamu TAKEDA** (*Gunma Univ. and IMS*), **Akira YAMAGUCHI** (*Univ. Tokyo*), **Tsunehisa OKUNO** (*Univ. Tokyo*), **Kunio AWAGA** (*Univ. Tokyo*) and **Kizashi YAMAGUCHI** (*Osaka Univ.*)

[*Mol. Cryst. Liq. Cryst.* in press]

Electron spin density distribution was investigated for *p*- and *m*-pyridyl nitronyl nitroxides (*p*-PYNN and *m*-PYNN) in the crystalline phase by the temperature dependence of the solid state high resolution ¹H-MAS NMR spectrum. The results were compared with that of phenyl nitronyl nitroxide (PNN) for elucidating the effect of incorporation of a nitrogen atom into the aromatic group. For *p*-PYNN, the magnitude of the negative spin density at 3 and 5 positions of the pyridyl group was suppressed by 30% in comparison with that of PNN and the positive spin density at 2 and 6 positions was slightly enhanced by 10%. On the other hand, the positive spin density at 2, 4 and 6 positions of

pyridyl group of *m*-PYNN was suppressed by 30% in average and the negative one at 5 was also suppressed by 20%. The DFT calculation at UBLYP/6-31G(d,p) level suggested that the molecular geometry largely contributed to the change of the spin density in addition to the effect of incorporation of the nitrogen atom. In fact, the spin density distribution of the aromatic ring of *p*-PYNN was remarkably reduced in solution compared with that in the crystalline phase.

IV-M-4 Solid State High Resolution Deuterium NMR Study of Electron Spin Density Distribution of Hydrogen-bonded Organic Ferromagnetic Compound 4-Hydroxyimino-TEMPO

Goro MARUTA (*Osaka Univ.*), **Sadamu TAKEDA** (*Gunma Univ. and IMS*), **Ron IMACHI** (*Univ. Electro-Commun.*), **Takayuki ISHIDA** (*Univ. Electro-Commun.*), **Takashi NOGAMI** (*Univ. Electro-Commun.*) and **Kizashi YAMAGUCHI** (*Osaka Univ.*)

Electron spin density distribution at hydrogen atoms of 4-hydroxyimino-2,2,6,6-tetramethylpiperidin-1-yloxy (4-hydroxyimino-TEMPO), which has been recently found to be a molecular ferromagnet at low temperature, was determined in the crystalline phase from the temperature dependence of the Fermi contact shifts of magic angle spinning deuterium NMR spectrum to elucidate the mechanism of intermolecular magnetic interaction. The plus and minus signs of observed hyperfine coupling constants A_D of methyl hydrogens revealed two different mechanisms of electron spin distribution. Equatorial CD₃ groups show negative coupling constants ($A_D = -0.24$ MHz) induced by the spin polarization mechanism, whereas positive hyperfine coupling constants ($A_D = +0.12$ MHz) of axial CD₃ groups indicate that single occupied MO spreads out partly toward the axial CD₃ groups by the mechanism of hyperconjugation. Large negative hyperfine coupling constant ($A_D = -0.45$ MHz) observed for NOD group implies that the spin polarization mechanism works via intermolecular hydrogen bond in the crystalline state. These experimental results and molecular orbital calculations indicate that there exists ferromagnetic interaction in the hydrogen bonded chains and these chains are coupled through the axial methyl groups.

IV-M-5 Local Magnetic Structure of Layered Compounds Cu₂(OD)₃X with Exchangeable Acid Anion X Studied by Solid State High Resolution Deuterium NMR

Sadamu TAKEDA (*Gunma Univ. and IMS*), **Goro MARUTA** (*Osaka Univ.*), **Katsumasa TERASAWA** (*Gunma Univ.*), **Nobuya FUKUDA** (*Gunma Univ.*) and **Kizashi YAMAGUCHI** (*Osaka Univ.*)

[*Mol. Cryst. Liq. Cryst.* in press]

The microscopic magnetic local structure of Botallackite-type layer structured compounds Cu₂(OD)₃X (X = NO₃⁻ and HCOO⁻) exhibiting non-

equilateral planar triangular magnetic lattice was determined by the solid-state high resolution deuterium NMR of deuterated hydroxy groups in the high temperature region above 190K. The magnetic interactions in a copper ion layer were probed by the paramagnetic NMR shifts of the two chemically distinct hydroxy groups. Isotropic NMR shift of each hydroxy group showed different temperature dependence, suggesting non-uniform magnetic interaction. It appeared that the magnetic interaction in the copper layer could

be decomposed to a sum of 1D-Heisenberg ferro- and antiferromagnetic chains in the high temperature region. Two distinct copper chains with ferro- and antiferromagnetic exchange interactions $J = +19 \pm 11$ and -21 ± 3 K were found for $X = \text{NO}_3^-$ from the temperature dependence of the two distinct NMR signals, while $J = +13 \pm 7$ and -13 ± 5 K for $X = \text{HCOO}^-$. The derived values of J almost reproduced the temperature behavior of the magnetic susceptibility χ vs. T .

IV-N Proton Transfer Tunneling in Interacting Hydrogen Bonds in the Solid State

Control of functional interactions, such as electronic and dynamic one, is a key to produce new functional materials. It is important to study the possibility of the functional interactions in the solid state. The nuclear magnetic resonance provides microscopic aspects of the functional interactions in the solid state. Hydrogen bond has a great capability for mediating a variety of interactions. We have investigated proton transfer dynamics in the interacting hydrogen bonds in organic quasi-conjugated π -system. Interaction between the hydrogen bonds is a key point for propagating an information of one hydrogen bond to the other hydrogen bond through molecular frame.

IV-N-1 Observation of Thermal Tautomerism of Thermochromic Salicylidene-Aniline Derivatives in the Solid State by ^{15}N CPMAS NMR down to Cryogenic Temperatures

Claudia BENEDICT (*Freie Univ. Berlin*), **Uwe LANGER** (*Freie Univ. Berlin*), **Hans-Heinrich LIMBACH** (*Freie Univ. Berlin*), **Hironori OGATA**, and **Sadamu TAKEDA** (*Gunma Univ. and IMS*)

[*Ber. Bunsenges. Phys. Chem.* **102**, 335 (1998)]

Temperature dependence of solid state ^{15}N -CP/MAS NMR spectra of ^{15}N enriched salicylideneaniline derivatives, *N*-salicylideneaniline (SA), *N,N'*-bissalicylidene-*p*-phenylenediamine (BSP) and *N,N'*-di(2-hydroxy-1-naphthylidene)-*p*-phenylenediamine (DNP) were measured in order to study possible proton transfer process in the NHO hydrogen bonds. For DNP a remarkable change of the ^{15}N chemical shift of more than 50 ppm was observed between 26 and 388 K by using the CP/MAS NMR technique down to cryogenic temperatures. The result clearly indicates very small enthalpy differences among the four tautomers associated with the combination of two possible forms, OH and NH forms, of the two NHO hydrogen bonds in a DNP molecule.

IV-N-2 Proton Dynamics in Interacting Hydrogen Bonds in the Solid State: Proton Tunneling in the NHO Hydrogen Bonds of *N,N'*-Di(2-hydroxy-1-naphthylmethylene)-*p*-phenylenediamine

Sadamu TAKEDA (*Gunma Univ. and IMS*), **Tamotsu INABE** (*Hokkaido Univ.*), **Claudia BENEDICT** (*Freie Univ. Berlin*), **Uwe LANGER** (*Freie Univ. Berlin*) and **Hans-Heinrich LIMBACH** (*Freie Univ. Berlin*)

[*Ber. Bunsenges. Phys. Chem.* in press]

Combination of comprehensive investigations of the spin-lattice relaxation rate of proton and low temperature ^{15}N -CP/MAS NMR spectrum provides unique information of proton dynamics in two interacting NHO hydrogen bonds of solid *N,N'*-di(2-hydroxy-1-naphthylmethylene)-*p*-phenylenediamine (DNP). It was evidenced from the ^1H -NMR relaxation measurement that tunneling mechanism operates for the proton transfer in the hydrogen bonds. The tunneling phenomenon is closely related to the very small energy differences among the four tautomeric states accompanied with the proton transfer in the two NHO hydrogen bonds. The very small values of the energy difference, in spite of the chemically asymmetric NHO hydrogen bond, were revealed by the ^{15}N -CP/MAS NMR spectrum. This is a unique character of solid DNP. It was also suggested from the derived energy scheme of the four tautomers and activation energies of the proton transfer that an interaction exists between the two NHO hydrogen bonds linked by π -electronic molecular frame. This means that the information of one NHO hydrogen bond, *e.g.* OH-form or NH-form, propagates to the other hydrogen bond and the proton transfer in one hydrogen bond induces the change of the potential function for the proton transfer in the other hydrogen bond.